



HAL
open science

The geological evolution of the Variscan Jebilet massif, Morocco, inferred from new structural and geochronological analyses

Sylvain Delchini, Abdeltif Lahfid, B. Lacroix, Thierry Baudin, C. Hoepffner, Catherine Guerrot, Philippe Lach, O. Saddiqi, Claire Ramboz

► To cite this version:

Sylvain Delchini, Abdeltif Lahfid, B. Lacroix, Thierry Baudin, C. Hoepffner, et al.. The geological evolution of the Variscan Jebilet massif, Morocco, inferred from new structural and geochronological analyses. *Tectonics*, 2018, 37 (12), pp.4470-4493. 10.1029/2018TC005002 . insu-01928494

HAL Id: insu-01928494

<https://insu.hal.science/insu-01928494v1>

Submitted on 19 Dec 2018

HAL is a multi-disciplinary open access archive for the deposit and dissemination of scientific research documents, whether they are published or not. The documents may come from teaching and research institutions in France or abroad, or from public or private research centers.

L'archive ouverte pluridisciplinaire **HAL**, est destinée au dépôt et à la diffusion de documents scientifiques de niveau recherche, publiés ou non, émanant des établissements d'enseignement et de recherche français ou étrangers, des laboratoires publics ou privés.



Tectonics

RESEARCH ARTICLE

10.1029/2018TC005002

Key Points:

- Extension and magmatism during latest Devonian to Early Carboniferous (D_0) are related to opening of the Paleotethys Ocean
- Late Carboniferous to Early Permian Variscan tectonics (D_1 , D_2) developed HT-LP metamorphism that cannot be explained by crustal thickening
- Moderate crustal thickening and HT-LP metamorphism can be explained by an inherited thermally weakened crustal domain

Supporting Information:

- Supporting Information S1
- Table S1
- Table S2

Correspondence to:

S. Delchini,
delchini.sylvain@gmail.com

Citation:

Delchini, S., Lahfid, A., Lacroix, B., Baudin, T., Hoepffner, C., Guerrot, C., et al. (2018). The geological evolution of the Variscan Jebilet massif, Morocco, inferred from new structural and geochronological analyses. *Tectonics*, 37. <https://doi.org/10.1029/2018TC005002>

Received 30 JAN 2018

Accepted 6 NOV 2018

Accepted article online 9 NOV 2018

The Geological Evolution of the Variscan Jebilet Massif, Morocco, Inferred From New Structural and Geochronological Analyses

S. Delchini^{1,2,3} , A. Lahfid^{1,2,3}, B. Lacroix⁴, T. Baudin¹, C. Hoepffner⁵, C. Guerrot¹ , P. Lach¹, O. Saddiqi⁶, and C. Ramboz²

¹BRGM, Orléans, France, ²CNRS, ISTO, UMR 7327, Orléans, France, ³Université d'Orléans, ISTO, UMR 7327, Orléans, France,

⁴Department of Geology, Kansas State University, Manhattan, KS, USA, ⁵Department of Geology, Faculty of Sciences,

Hon. Pr. Mohamed V University, Rabat, Morocco, ⁶Department of Geology, Faculty of Sciences Ain Chock, Hassan II University of Casablanca, Casablanca, Morocco

Abstract The present work aims at understanding the tectonic evolution of the Jebilet massif, Morocco, during the Late Paleozoic as constrained by structural, metamorphic, and geochronological studies. From Late Devonian to Early Carboniferous, bordering faults controlled the opening of the Jebilet intracontinental basin (D_0 stage) as shown by sedimentary infill. This episode was accompanied by a magmatic activity, newly dated between 358 ± 7 Ma and 336 ± 4 Ma. The first record of the Variscan event affected the Jebilet by the Late Visean-Namurian and is represented by allochthonous superficial nappes emplaced at shallow depth in a moderately lithified sedimentary succession. D_1 also developed regional-scale recumbent folds trending E-W that may suggest N-S crustal shortening not generating crustal thickening nor contributing to metamorphism. The main Variscan D_2 episode⁴ consists of a progressive evolution from bulk coaxial deformation to noncoaxial dextral transpression consistent with NW-SE horizontal shortening, resulting in a moderate thickening. This episode was accompanied by HT-LP metamorphism and syntectonic intrusions controlled by an inherited thermal anomaly in relation with the intracontinental rifting stage (D_0). Based on previous age determinations from syntectonic leucogranite and metamorphic rocks, D_2 is dated between 310 and 280 Ma. The tectono-metamorphic evolution of the Jebilet massif can be correlated with a plate-tectonic scenario evolving from, first a Late Devonian-Early Carboniferous basin formation during stretching of the north-Gondwana margin and initiation of the Paleotethys Ocean, and, second, to a Late Carboniferous-Early Permian ocean closure (Rheic or Paleotethys Oceans depending of scenarios) that resulted in the final Variscan-Alleghanian tectonics.

1. Introduction

The Moroccan Meseta Domain (MMD), surrounded by discordant Mesozoic and Cenozoic formations, was part of the northern margin of the Gondwana supercontinent and is considered as the south-western external part of the Variscan-Alleghanian belt (Hoepffner et al., 2005, 2006; Michard et al., 2010). It exposes a nearly complete Paleozoic sedimentary succession, folded and intruded by widespread preorogenic, synorogenic to late-orogenic magmatism related to different events that occurred during the Variscan-Alleghanian collision between Gondwana-derived continental blocks and Laurussia (Hoepffner et al., 2005, 2006; Michard et al., 2010). The MMD, located far from convergent plate boundaries, was affected by Late Carboniferous to Early Permian deformation and metamorphism. No consensus has yet been reached to explain the tectonic evolution responsible for the MMD structures. Previous work (Hoepffner et al., 2005, 2006; Michard et al., 2008, 2010; Piqué et al., 1980) suggested that the MMD corresponds to an intracontinental orogen with its own tectonic evolution, characterized during the main Late Carboniferous to Early Permian Variscan event by a single W-E to NW-SE compression. This heterogeneous polyphase deformation would have developed in a collisional-transpressional context, controlled by crustal ductile shear zones like the Western Meseta Shear Zone (WMSZ).

Recently, based on structural analysis coupled with geochronological data in the Rehamna massif, Chopin et al. (2014) proposed another tectonic evolution model for the MMD, caused by a change in orientation of the main tectonic stresses. This change would have induced two distinct compressional events: first, a

Late Carboniferous N-S compressional deformation resulting in crustal thickening and folding by allochthonous nappe stacking, followed by an Early Permian orthogonal NW-SE transpressional event refolding the older (phase-1) structures.

Several works highlight the close relationship between the tectonic evolution of the Jebilet massif and that of the Rehamna massif, located 40 km farther north (Hoepffner et al., 2006; Michard et al., 2010). Since the work of Huvelin (1977), the Jebilet massif has been extensively studied and its current architecture is considered to be the result of a single post-Visean NW-SE transpressional deformation stage (Bordonaro et al., 1979; Essaifi et al., 2001, 2003, 2013; Gaillet & Bordonaro, 1981; Huvelin, 1977; Lagarde, 1985; Le Corre & Bouloton, 1987).

Despite all this structural work, the tectonic evolution of the Jebilet massif is still incompletely constrained and remains controversial. For instance, it is characterized by significant magmatic activity whose origin, tectonic setting, and age of emplacement are still debated. Magmatism could correspond either to a preorogenic extensional setting where tholeiitic-affinity magmas emplaced in a continental rift-type basin (Aarab, 1984, 1995; Aarab & Beauchamp, 1987; Bordonaro, 1983; Bordonaro et al., 1979; Jadid, 1989) or to a synorogenic transpressional setting where magmas emplaced synchronously with the major tectono-thermal event (Essaifi et al., 2003; Lagarde & Choukroune, 1982; Le Corre & Saquaque, 1987). Another controversial issue concerns the processes of allochthonous nappe emplacement in the Jebilet massif, which are considered either as synsedimentary (gravitational) related to an extensional tectonic setting (Bamoumen, 1988; Hollard et al., 1977; Huvelin, 1977) or as tectonic, that is, formed in front of an accretionary wedge (Graham, 1982a; Zahraoui, 1981).

The aim of our paper is to clarify the tectonic evolution of the Jebilet massif from the Late Devonian to the Early Permian to better understand the geological history of the MMD. To address this issue, we have combined new structural and petrologic observations with new U-Pb age data (laser ablation inductively coupled plasma-mass spectrometry or LA-ICP-MS, BRGM), together with pertinent data from the literature. This combined analysis has allowed us to understand both the complex tectonic processes, and the chronology of magma emplacement, responsible for the Jebilet evolution during the Late Paleozoic. These new results provide not only a better understanding of the MMD tectonic evolution in the framework of the Variscan-Alleghanian orogeny but also new discussion elements concerning the mechanisms involved in this tectonic evolution.

2. Geological Setting

The Jebilet massif, located north of Marrakech and the High Atlas, belongs to the western Moroccan Meseta (Figure 1a) and, like other massifs of the Meseta, consists of folded Paleozoic rocks surrounded by discordant Mesozoic and Cenozoic formations. It is traditionally divided into the Western, Central, and Eastern Jebilet, characterized by distinct lithological, magmatic, tectonic, and metamorphic features (Huvelin, 1977), and separated by major shear zones (Figures 1b and 2). The Western and Central Jebilet are separated by the NNE-SSW trending WMSZ (Le Corre & Bouloton, 1987; Piqué et al., 1980), whereas the boundary between the Central and Eastern Jebilet corresponds to the sinistral NNW-SSE Marrakech Shear Zone (Essaifi et al., 2001; Lagarde & Choukroune, 1982).

The Jebilet massif consists of an almost complete Paleozoic sedimentary succession, overlying a Pan-African basement with Eburnean components as inferred by the U-Pb dating of zircons extracted from xenoliths in Triassic dykes, yielding 2,000 Ma, 700 Ma, 615–540 Ma, and 328–280 Ma ages (Dostal et al., 2005).

The succession starts with Early Cambrian archeocyathes limestone in the Western Jebilet, belonging to the Meseta Coastal Block. This limestone is overlain by a thick series of Middle Cambrian to Ordovician detrital sediments, including Middle Cambrian magmatic effusive rocks (Huvelin, 1977); this volcanism is associated with the synsedimentary NNE trending normal faults linked to the opening of the Rheic Ocean (Bernardin et al., 1988; Mayol, 1987). Silurian deposits are lacking in the Western Jebilet, probably due to erosion before the Devonian, but the Devonian itself consists of a transgressive series of red conglomerate, massive limestone, and quartzitic sandstone (Tahiri, 1982). The lack of Carboniferous deposits is explained by emersion of the Western Jebilet during this period (Piqué, 1979) and may be partly the result of post-Variscan erosion of the folded chain. At its eastern boundary (the only one shown in Figures 1b and 2), the Western Jebilet is marked by the Early Cambrian Bou Gader Formation, which is stratigraphically overlain by the *disorganized*

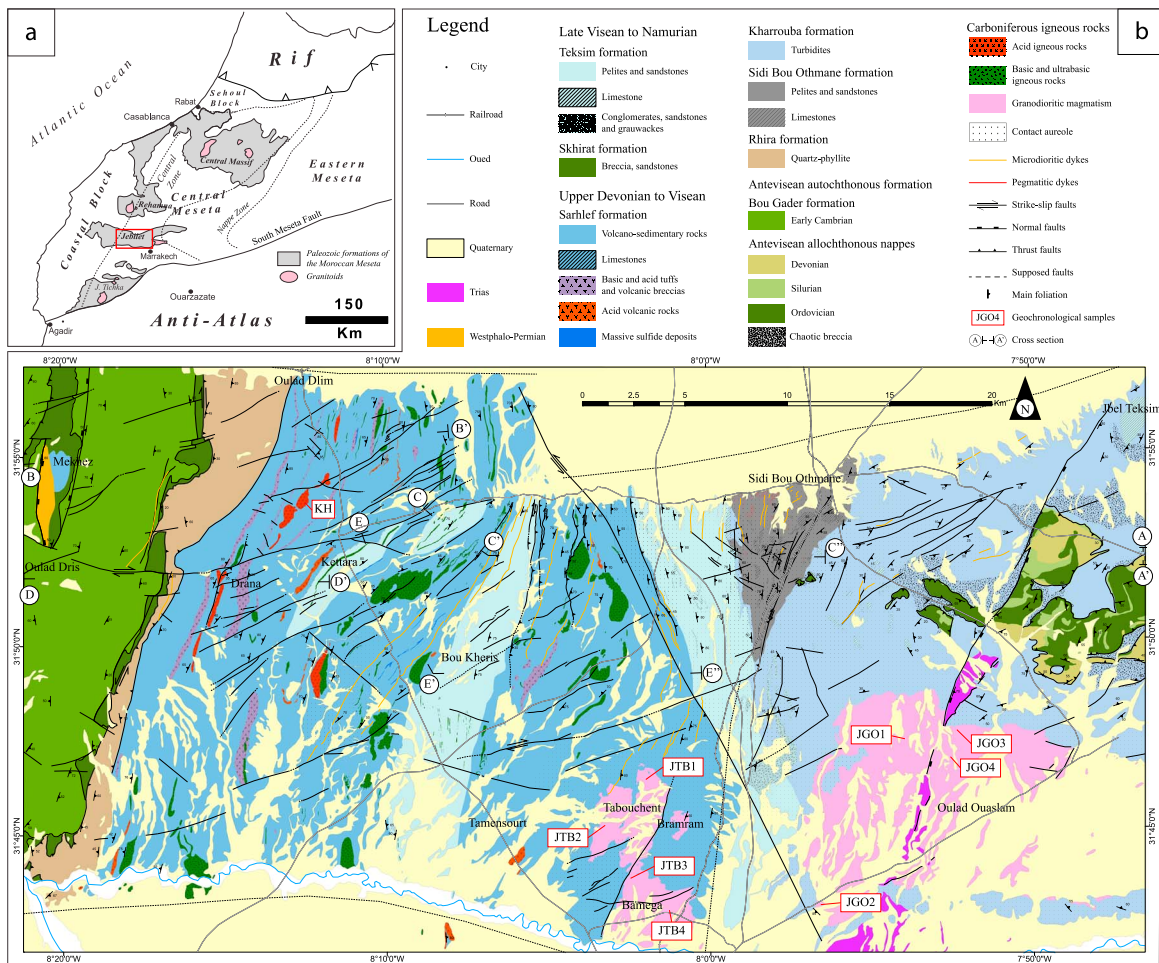


Figure 1. (a) Location of the Jebilet massif. (b) Geological map of the studied area based on our field observations and on previous studies (Bernard et al., 1988; Bordonaro, 1983; El Hassani, 1980; Gaillet & Bordonaro, 1981; Graham, 1982a; Huvelin, 1977; Mayol, 1987; Zahraoui, 1981) and location of the cross-sections on Figures 3a and 6.

Skhirat Formation: a breccia constituted by Ordovician, Devonian, and Viséan blocks derived from the western part of Coastal block (Mayol, 1987).

The Central and Eastern Jebilet are supposedly formed by Devonian-Carboniferous sedimentary rocks (Hollard et al., 1977; Huvelin, 1977; Mayol, 1987). However, due to the intense metamorphism, deformation, and very few paleontological and isotopic age determinations in this area, the lithostratigraphy still remains uncertain, as is shown by the many different interpretations of the chronological and spatial relationships (Aarab & Beauchamp, 1987; Bordonaro, 1983; Gaillet, 1979; Hollard et al., 1977; Huvelin, 1977; Mayol, 1987; Sougy, 1976). For this reason, we provide in the following paragraphs a detailed description of the stratigraphic succession of the Central and Eastern Jebilet, and their chronological and spatial relationships.

The lithostratigraphic succession of the Eastern Jebilet is subdivided into the three Sidi Bou Othmane, Kharrouba, and Teksim formations (Figures 1b and 2), whose stratigraphic relationships are unclear. The Sidi Bou Othmane Formation is probably overlain by the Kharrouba Formation, but their spatial relationship is still difficult to establish due to the intensity of both metamorphism and deformation. The transgressive Teksim Formation conformably overlies the Kharrouba Formation (Beauchamp, 1984; El Hassani, 1980; Gaillet, 1979; Graham, 1982a, 1982b; Huvelin, 1977; Izart et al., 1997; Zahraoui, 1981).

The Sidi Bou Othmane Formation, whose base is unknown, is mainly composed of graphite-rich limestone interlayered with quartzite and shale (El Hassani, 1980). Although the absolute age of this formation is unknown, Huvelin (1977) and El Hassani (1980), based on lithological correlation with the Teksim

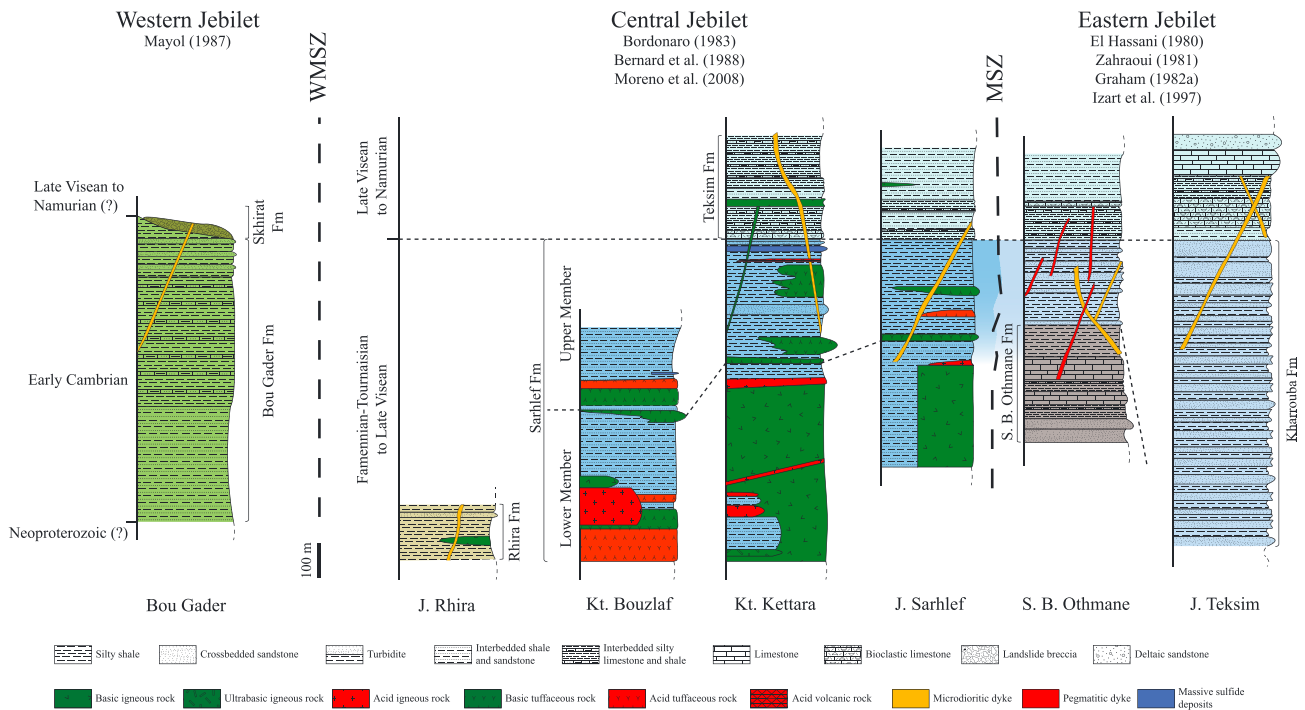


Figure 2. Synthetic lithostratigraphic logs of the Jebilet massif for each tectonic domain (Western, Central and Eastern Jebilet) based on previous studies (Beauchamp, 1984; Bernard et al., 1988; Bordonaro, 1983; El Hassani, 1980; Huvelin, 1977; Izart et al., 1997; Mayol, 1987; Moreno et al., 2008; Zahraoui, 1981) and refined by our field observations.

Formation, attributed this formation to the Late Viséan-Namurian. However, considering the probable position of this formation below the Kharrouba Formation, as well as the regional metamorphic amphibolite facies, a Late Devonian to Early Carboniferous age is also proposed (Figure 2; Delchini et al., 2016).

The base of the Kharrouba Formation is unknown, but its exposed part is characterized by laminated shales that gradually evolve to sandstone beds, marking the transition toward an overlying thick turbidite deposit dated Middle Viséan (Cf5 of Izart et al., 1997). The turbidites are covered by platform deposits characterized by slump facies alternating with shale and siltite and evolving toward turbidite/tempestite sandstone. At the top of Kharrouba, the turbidite/tempestite sandstone gradually passes to fossiliferous green platform shale dated Late Viséan to Namurian (Cf6 of Hollard et al., 1977; Huvelin, 1977). Several alkaline volcanic (pillow-lava, sills, hyaloclastite, and spilite) and volcano-sedimentary (interstratified pyroclastic breccias) units are described from the Kharrouba Formation (Bamoumen et al., 2008; Huvelin, 1977).

The uppermost Teksim Formation consists of Late Viséan transgressive carbonate-dominated sandy limestone and bioclastic/oolitic reefal limestone (Figure 2; V3b of Hollard et al., 1977; Cf6 γ of Beauchamp, 1984). These are overlain by prograding deltaic sandstone and conglomerate, possibly of Namurian age by correlation with the stratigraphy of the High Atlas (Cf7 of Beauchamp, 1984).

In the Eastern Jebilet, a notable feature is the presence of Ordovician to Devonian allochthonous nappes thrust over an extensive chaotic breccia with Ordovician to Late Viséan clasts, up to several tens of meter-thick (Figure 1b). The processes leading to emplacement of the allochthonous nappes and chaotic breccia formation are still debated and considered either as an olistostrome resulting from submarine gravitational mass transport (syndimentary origin; Bamoumen et al., 2008; Hollard et al., 1977; Huvelin, 1977) or as a tectonic nappes (Graham, 1982a; Zahraoui, 1981). Due to the existence of these nappes, whose emplacement was Late Viséan-Namurian, or slightly younger depending on whether they are syndimentary or tectonic, the Eastern Jebilet has been attached to the Nappe Zone of the Meseta domain (Figure 1a), (Hoepffner et al., 2005; Michard et al., 2010).

The Central Jebilet (Figures 1b and 2) represents the western part of the supposed Devonian-Carboniferous basin of the Jebilet, in broad continuity with the eastern part as shown by the overlying Late Viséan-Namurian

calcareous Teksim Formation on the Sarhlef series (Bordonaro et al., 1979; Gaillet, 1980; Gaillet & Bordonaro, 1981). The Sarhlef series is considered as a lateral equivalent of the Kharrouba Formation (Bordonaro et al., 1979; Gaillet & Bordonaro, 1981). It has a minimum estimated thickness of 1,000 m and is subdivided into a *Lower Member* and an *Upper Member* (Figure 2; Belkadir et al., 2008; Bernard et al., 1988; Bordonaro, 1983; Moreno et al., 2008). The Lower Member represents a distal facies including shale, sandstone, and felsic and mafic tuff with rapid lateral variations and is intruded by a bimodal association of tholeiitic mafic-ultramafic and alkaline acidic plutons (see next section; Bernard et al., 1988; Bordonaro, 1983; Essaifi et al., 2003; Huvelin, 1977). The Upper Member was deposited on a proximal platform environment and consists of shale, siltstone, sandstone, and minor felsic volcanic rocks with lateral facies changes between coherent rhyodacite and volcanoclastic rocks (Koudiat Delaa, Draa Sfar). The Upper Member hosts massive sulfide mineralization (e.g., the Kettara and Draa Sfar mines). The Draa Sfar pyrrhotite-rich, polymetallic massive sulfide deposit is considered as Late Visean, based on a palynological analysis (Huvelin, 1977; Moreno et al., 2008; Playford et al., 2008), which was confirmed by Ar-Ar dating (yielding an age of 331.7 ± 7.9 Ma) of hydrothermal sericite in rhyolite below the Draa Sfar deposit (Marcoux et al., 2008). The western margin of the Central Jebilet (Figures 1b and 2) is characterized by quartz phyllites corresponding to the Rhira Formation of probable Late Devonian age (Famennian, by correlation with exposures in the Rehamna massif) and separated from the Sarhlef Formation by late tectonic contacts (Bordonaro, 1983; Bordonaro et al., 1979).

The main magmatic bodies in the Jebilet massif (Figures 1b and 2) consist of a bimodal association of tholeiitic mafic-ultramafic and alkaline felsic stocks, dykes, or sills; (b) calc-alkaline granodioritic plutons, and (c) lamprophyric dykes. The bimodal plutonism (>65% mafic-ultramafic, the remainder being felsic) is only found in the Central Jebilet (Figures 1b and 2) and is represented by several felsic and mafic-ultramafic intrusions (hundreds of meters wide and a few kilometers long) intruding the Lower Member of the Sarhlef Formation (Bernard et al., 1988; Bordonaro, 1983; Essaifi et al., 2013; Huvelin, 1977). Mafic-ultramafic igneous rocks are represented by ultramafic cumulates, gabbro, and dolerite, locally altered to chlorite schist along the deformed zone (Essaifi et al., 1995). These stocks, even the largest kilometer-sized one, did not generate significant contact metamorphism (Huvelin, 1977). Felsic plutonic rocks are alkaline monzonitic microgranites, locally highly deformed and metasomatized to gneissic trondhjemite and tonalite. They crop out as dykes, stocks, and mainly as elongated intrusions forming the BHD lineament of Essaifi et al. (2004), inducing a contact metamorphism that reached hornblende-hornfels facies (Essaifi et al., 2001, 2013). One acidic intrusive stock of the BHD lineament was dated 330.5 ± 0.68 – 0.83 Ma (ID-TIMS U-Pb on zircon; Essaifi et al., 2003).

The large granitoid massifs consist of the two Oulad-Ouaslami and Bamega-Tabouchent calc-alkaline peraluminous plutons (Figure 1b), crosscut by leucogranitic stocks and dykes, and the Bramram pluton. The first two plutons are biotite \pm cordierite-bearing granodiorite with modal compositions ranging from monzogranite to tonalite (Bensalah, 1989; Rosé, 1987) and were dated at 327 ± 4 Ma (Rb-Sr: Mrini et al., 1992). The Bramram stock is a two-mica leucogranite with a crustal origin and was dated at 297 ± 9 Ma, 296 ± 6 Ma (Tisserant, 1977), and 295 ± 15 Ma (Mrini et al., 1992) using the Rb-Sr method on whole rock. The emplacement of the granodiorite intrusions was accompanied by contact metamorphism in the pyroxene-hornfels facies (Bouloton, 1992; El Hassani, 1980; Huvelin, 1977). The mineral assemblage in the metamorphic aureole indicates a pressure of ~ 2.2 kbar or a maximum depth of 8 km (Bouloton, 1992).

Finally, the youngest magmatic event in the area is represented by a dense array of lamprophyric dykes (Figures 1b and 2), intersecting both the earlier magmatic rocks and the folded metasediment rocks (Bouloton & Gasquet, 1995; Huvelin, 1977). Their mineralogical, petrological, and geochemical compositions display the characteristics of calc-alkaline to alkaline magmas. They were dated at ~ 255 Ma (K-Ar on amphibole) and at 235 ± 8 Ma (SHRIMP U-Th-Pb on zircon) and attributed to Atlantic prerifting (Dostal et al., 2005; Youbi et al., 2001).

Today's structure of the Jebilet massif is interpreted as resulting from a Late Devonian to Late Visean/Namurian extensional/transensional phase, characterized by large instabilities and disorganization shown by huge thickness and lithology variations controlled by strike-slip and normal faults. Most authors attributed the allochthonous nappe emplacement in the Eastern Jebilet to this event and considered it as synsedimentary (Bamoumen et al., 2008; Beauchamp & Izart, 1987; Hoepffner et al., 2006; Huvelin, 1977), but Graham (1982a) and Zahraoui (1981) argued for a tectonic emplacement, indicating that the nappe-setting process is not yet clearly established.

During the Westphalian to Permian, a transpressive heterogeneous deformation generated kilometer- to meter-scale N to NNE trending folds and local thrusts, associated with conjugate shear zones attesting to WNW-ESE to NW-SE shortening (Bouloton & Le Corre, 1985; Essaifi et al., 2001; Lagarde, 1985; Lagarde et al., 1989; Lagarde & Choukroune, 1982; Le Corre & Bouloton, 1987). This transpressive event was accompanied by a regional metamorphism in the greenschist to amphibolite facies and by syntectonic leucogranitic intrusions inducing a hornblende-hornfels facies contact-metamorphism (Bordonaro, 1983; Delchini et al., 2016; El Hassani, 1980; Huvelin, 1977). Based on structural analyses, some authors suggested that bimodal and granodiorite crystallization, dated around 330 Ma, was synkinematic of this transpressive event and synchronous of the major tectono-metamorphic phase (Essaifi et al., 2001, 2013; Lagarde et al., 1989; Lagarde & Choukroune, 1982). However, others (Aarab, 1984, 1995; Aarab & Beauchamp, 1987; Bordonaro, 1983; Bordonaro et al., 1979; Jadid, 1989) suggested that the plutonism occurred during the extensional/transensional phase.

This controversy clearly shows that the tectonic setting of the bimodal and granodioritic magmatism is still debated and needs geochronological data providing constraints on its timing.

During post-Variscan times, the Jebilet massif underwent extensional faulting and moderate burial related to the breakup of Pangea from the Early Permian to the Early Jurassic. This was followed by Jurassic to Early Cretaceous uplift and erosion, in turn followed by shallow burial up to the middle Eocene (Ghorbal et al., 2008; Saddiqi et al., 2009). The whole massif was finally uplifted during the Atlas orogeny as the hanging wall of the major post-middle Eocene south-dipping North-Jebilet reverse fault (Hafid, 2006; Hafid et al., 2008).

The absence of precise chronological and spatial relationships between the formations of the Jebilet massif and the limited number of age determinations realized on Jebilet plutonic rocks are at the origin of the still unresolved controversies mentioned above. However, our field observations and structural analyses question the role of a collisional-transpressional regime as the unique tectonic event responsible for the actual architecture of the Jebilet massif. Thus, in order to better constrain the complex geological history of the Jebilet and its tectono-metamorphic evolution from Late Devonian to Permian, we carried out the following: (1) a review of available structural and metamorphic data on the Jebilet massif, coupled with our field observations and structural analyses, and (2) a geochronological study of the main plutonic rocks.

3. Structural Analysis

Based on our fieldwork, three main tectonic phases (D_0 , D_1 , and D_2) of variable intensity now are distinguished in the Jebilet massif.

3.1. D_0 Event

The first D_0 phase corresponds to an extensional and/or transtensional period of rifting in the Jebilet massif that occurred from the Famennian (Rhira Formation) until the Late Visean-Namurian (Teksim Formation). During this period of rifting, the basement was affected by two distinct sets of normal faults oriented roughly NNE and ENE, with a transcurrent component and controlling the sedimentation as shown by synsedimentary thickness variations produced by block tilting (Aarab & Beauchamp, 1987; Bamoumen, 1988; Bamoumen et al., 2008; Huvelin, 1977).

3.2. D_1 Structures

D_1 structures consist of kilometer- to meter-scale tight recumbent folds (F_1), mainly visible in the eastern part of the Eastern Jebilet, in the Kharrouba, and Teksim formations (Figures 1b and 3a and 3b and 3e). D_1 structures are also seen in the allochthonous nappes of the Eastern Jebilet as shown on the cross section of Figure 3a characterized by a kilometer-scale recumbent F_1 fold with northward vergence in Devonian rocks. A chaotic breccia forms the contact zone between the autochthonous Teksim Formation and the base of the allochthonous Devonian nappe (Figures 3a and 3c). This breccia consists of centimeter-long blocks of both autochthonous and allochthonous formations and is embedded in a fine-grained matrix (Figure 3c). The blocks have an elongated shape parallel to the fine-grained matrix fabric, showing that the chaotic breccia is of tectonic origin. Away from the fault zone and tectonic breccia, both allochthonous Devonian and autochthonous Teksim rocks display well-bedded strata presenting in situ boudin structures associated with fractures and extensional veins (Figures 3a and 3d), indicating disruption of moderately lithified sediment at a

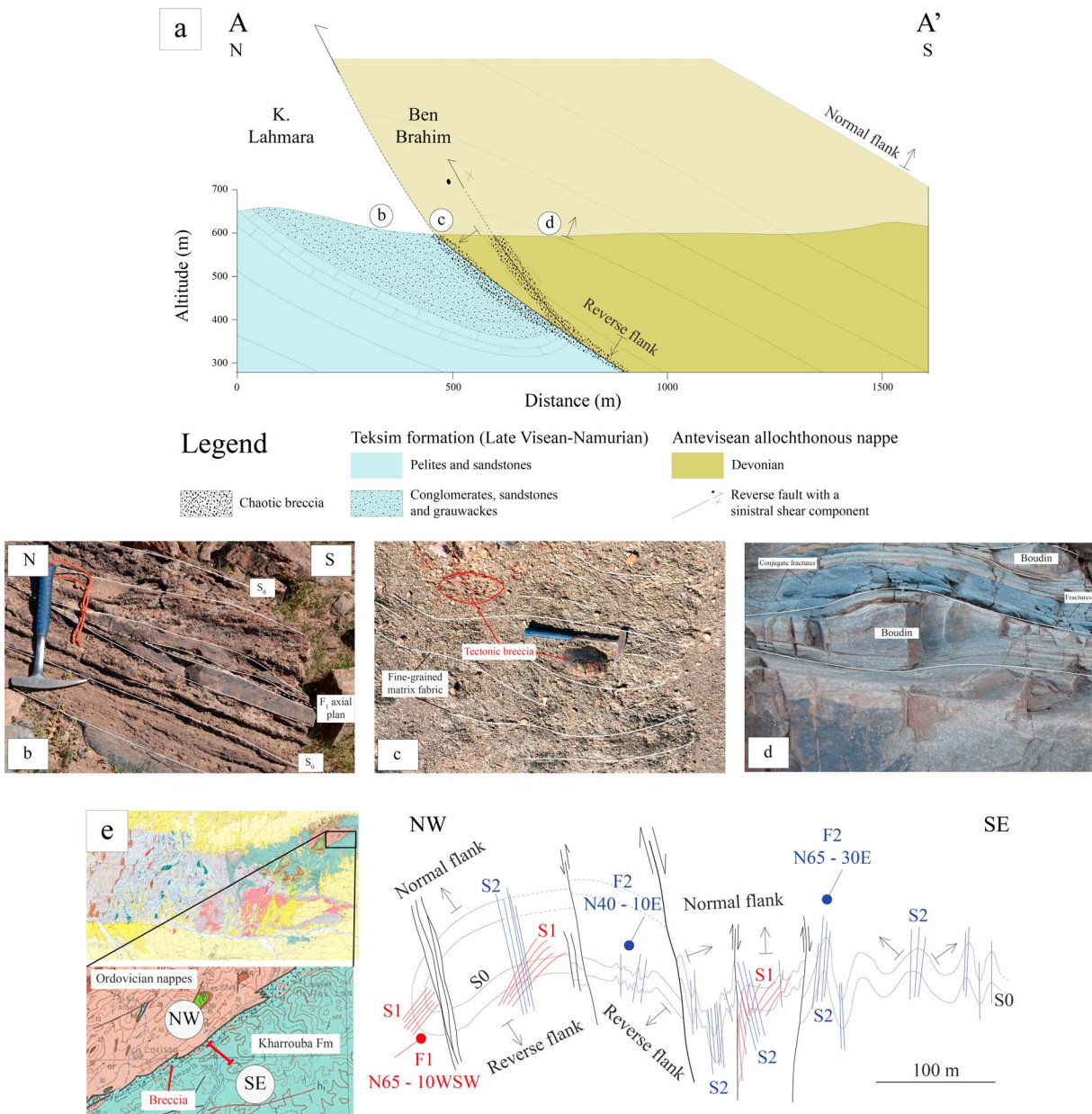


Figure 3. (a) Interpretative geological cross section presenting D1 deformation characterized by F1 recumbent folds respectively in the Devonian nappes and in the Teksim Formation in the Eastern Jebilet; see location in Figure 1b. (b) Meter-scale F1 recumbent fold in the Teksim Formation. (c) Tectonic breccia related to D1 thrust faulting at the base of the allochthonous nappes. (d) Subhorizontal boudin associated with fractures formed by strata disruption in the allochthonous Devonian rocks. (e) Schematic cross section based on observations by Zahraoui (1981), showing the S1/S2 cleavage relation in the Fokra-Messaoud area, located east of our study area; he found that the Kharrouba Formation is involved in a recumbent fold with north-west vergence.

high structural level. These shallow-depth structures also explain the absence of regional-scale S_1 cleavage in this unmetamorphosed sedimentary series of the eastern part of Eastern Jebilet (Figure 1b). As folding affects both the Kharrouba and the Teksim formations, and as the tectonic breccia is composed of Teksim Formation clasts, the D₁ deformation postdates the Late Visean to Namurian (325 Ma).

These structural observations agree with the ones by Zahraoui (1981) in the Fokra-Messaoud area, east of our study area (Figure 3e). Based on sedimentary polarity and S_1/S_2 cleavage chronology, this author showed that the Kharrouba Formation is involved in a recumbent fold with a north-west vergence (Figure 3e). Altogether, our structural data, coupled with those of Zahraoui (1981) and Bamoumen (1988), show that F₁ folds are very dispersed trending from N000 to N090 (Figure 4a) with various senses of vergence (west, south, south-east,

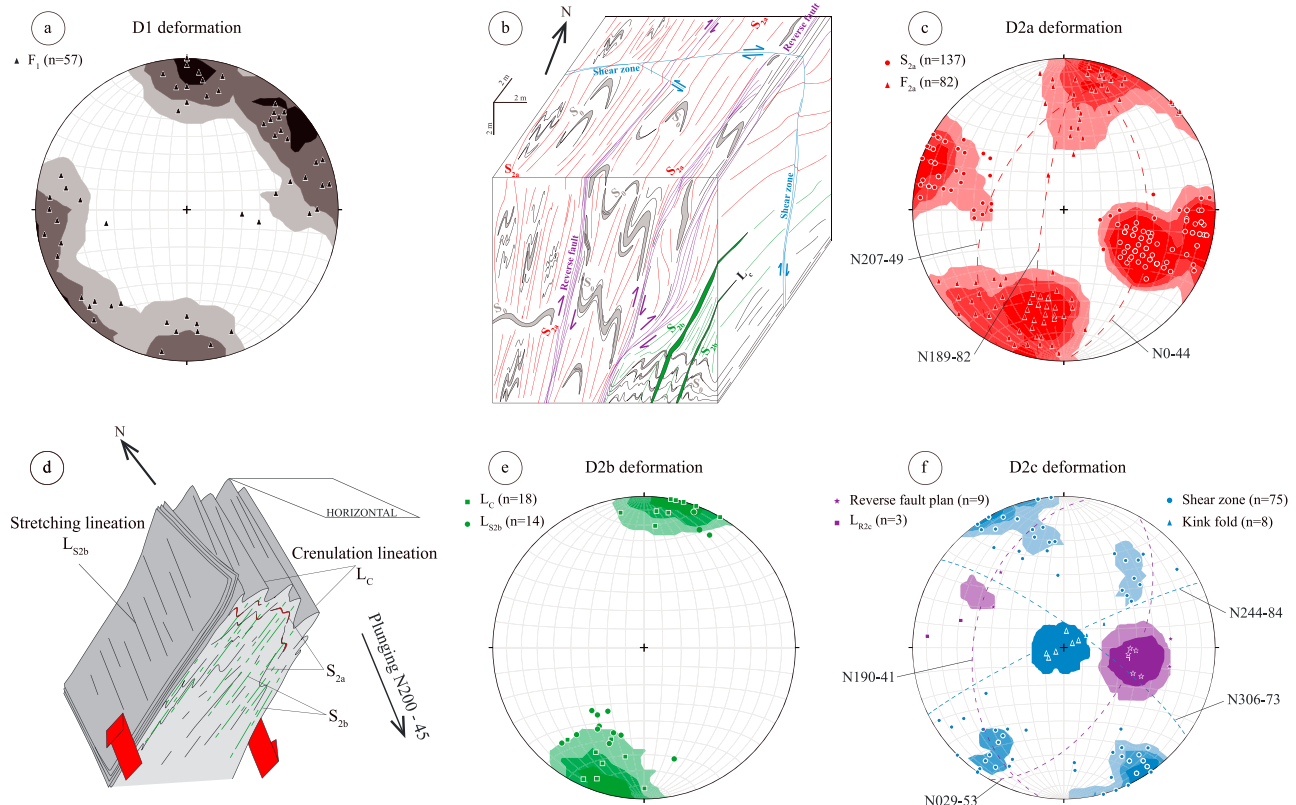


Figure 4. Three-dimensional sketch and stereographic diagrams (equal area, lower hemisphere projections) of planar and linear structures. (a) Density diagrams of the F₁ fold axes in the Eastern Jebilet. (b) Three-dimensional sketch to explain D₁ and D₂ relationships. (c) Density diagrams of the S_{2a} foliation poles and the F_{2a} fold axes in the Jebilet massif. As shown by the red dashed lines, S_{2a} axial plane foliation dip has a mean value of N189°–82°W in the major part of the Jebilet massif, except in the west-Central Jebilet and in the Sidi Bou Othmane area where it dips respectively to the east (N000°–44°E) and to the west (N207°–49°W). (d) Three-dimensional sketch showing S_{2a}/S_{2b} relationships. (e) Density diagrams of L_c crenulation lineation and L_{S2b} stretching lineation in the Jebilet massif. (f) D_{2c} strain pattern in the Jebilet massif characterized by reverse faults with LR_{2c} stretching lineation and conjugate strike-slip shear bands network with subvertical kink folds axes. As shown by the purple dashed line, the reverse faults trend NNE with a dip either toward the west (N190°–41°W) in the region of Sidi Bou Othmane, or toward the east (N029°–53°E) elsewhere in the Jebilet massif. As shown by the blue dashed line, strike-slip shear zones trend dominantly at N244–84°NW (dextral sense of shearing), whereas those of the subsidiary set preferentially trend at N306°–73°NE (sinistral sense of shearing).

north-west, and north). These structural data do not allow a precise determination of the initial trend and vergence of the D₁ structures in this part of the Eastern Jebilet, due to intense reworking by the D₂ event.

Nevertheless, in the Central Jebilet and in the west part of the Eastern Jebilet (Sidi Bou Othmane area), we locally identified D₁ deformation expressed by rare isoclinal F₁ folds refolded by D₂ deformation, transposing S₀ into a subvertical position (Figures 4b and 5a–5c). Here our field observations clearly showed that F₁-fold dispersion is compatible with an E-W orientation (Figures 4b and 5a–5c). Indeed, considering the roughly E-W shortening direction of the D₂ event as shown by stereograms (Figure 4c), a more or less E-W initial orientation of the F₁ folds seems consistent with the dispersion of D₁ fold axes by the D₂ event.

3.3. D₂ Structures

In our study area, the regionally dominant deformation D₂ is not homogeneously distributed and shows a dominant westward gradient of decreasing strain, as illustrated by the cross sections B-B' and D-D' on Figure 6.

D₂ is a polyphase deformation with three superimposed episodes, D_{2a}, D_{2b}, and D_{2c} that represent a continuum of deformation. D_{2a} deformation caused the large-scale refolding of F₁ folds along broad N-S to NNE trending isoclinal F_{2a} folds with an S_{2a} axial plane foliation (Figures 4b and 4c, 5c and 5d, and 6 and 7a). S_{2a} has variable dip with a mean value of N189°–82°W in most of the Jebilet massif, except in the west-Central Jebilet and in the Sidi Bou Othmane area where it dips respectively to the east (N000°–44°E) and to the west (N207°–49°W; Figure 4c). Figure 5b presents a structural analysis of the D₁–D_{2a} pattern

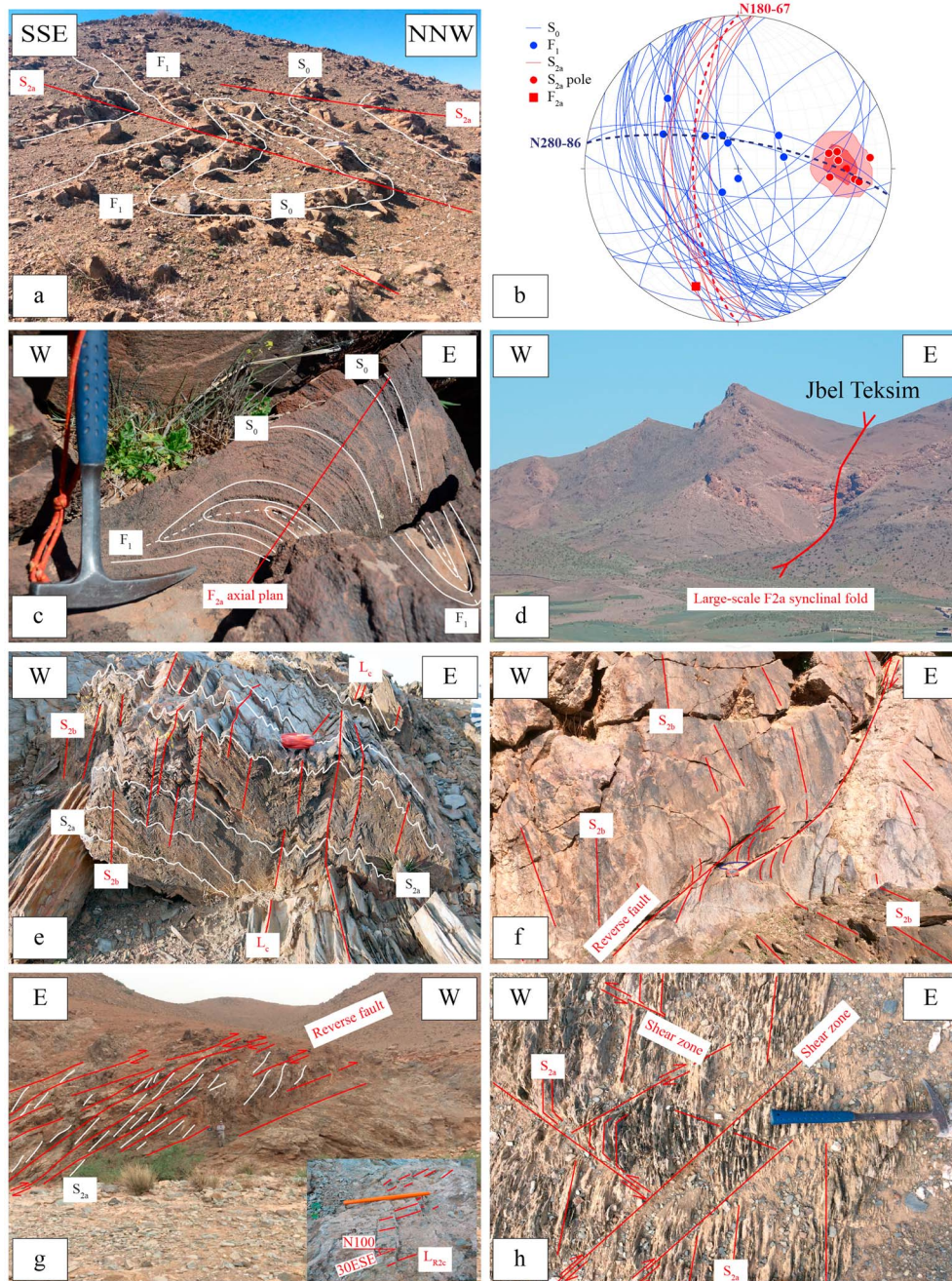


Figure 5. Field photographs and stereographic diagram presenting D1 and D2 relationships and D2 deformation structures in the Jebilet massif. (a–c) F1 isoclinal folds refolded by F2 up-right folds in the Sidi Bou Othmane Formation and stereographic projections (b) corresponding to (a). (d) Large-scale F2a folding in the Teksim Formation (Jebel Teksim area). (e) S2a foliation overprinted by a well-developed S2b crenulation cleavage in the Central Jebilet. (f and g) D2c reverse faults respectively in the Sidi Bou Othmane area and in the Drana area. (h) D2c shear zone network in the Central Jebilet (horizontal view).

interference of Figure 5a. The stereographic projection on Figure 5b shows that the S_0 plane distribution resulted in an F_{2a} axis around $N190^{\circ}\text{--}30^{\circ}\text{S}$, which agrees with the scattering of measured F_1 fold axes in the field, aligning along a great circle normal to the F_{2a} axis measured at $N190^{\circ}\text{--}14^{\circ}\text{S}$, with an axial plane foliation S_{2a} at $N180^{\circ}\text{--}67^{\circ}\text{W}$ (Figure 5b). F_{2a} folds and S_{2a} foliation were overprinted and reworked by a well-developed crenulation corresponding to D_{2b} deformation (Figures 4b, 4d, and 4e and 5e). The crenulation lineation L_c has a NNE trend and the axial planes are marked by an S_{2b} cleavage that forms a low angle with S_{2a} (Figures 4d and 4e and 7b–7e). The crenulation cleavage must be interpreted as a late

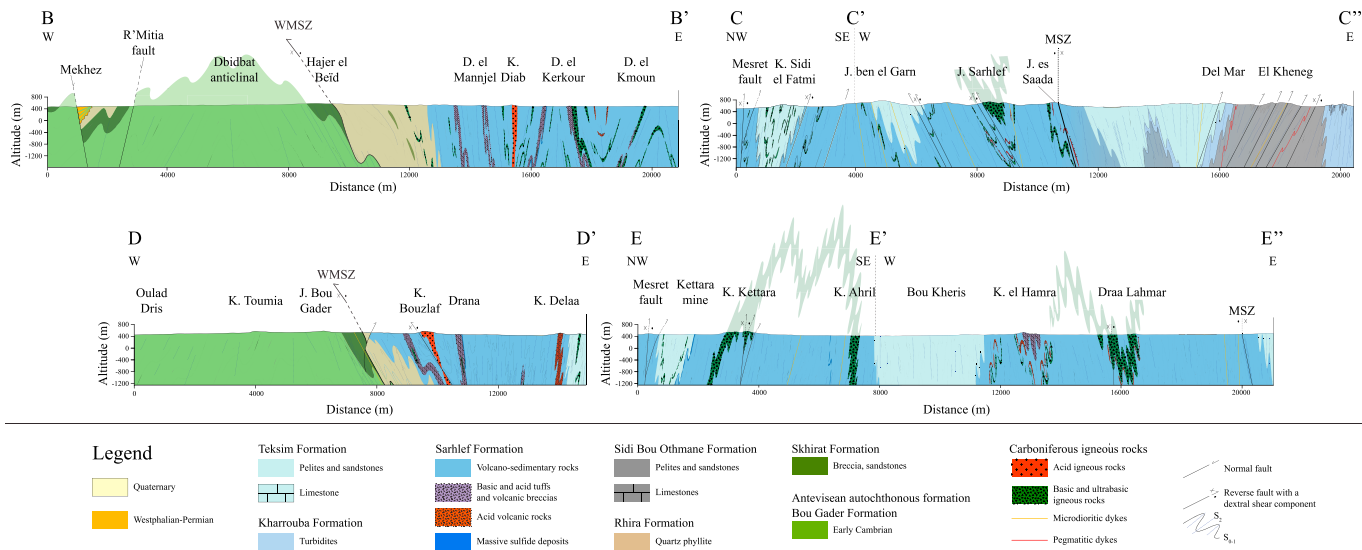


Figure 6. Interpretative geological cross sections presenting D₂ deformation in the Central Jebilet. See Figure 1 for localization.

increment of D₂. The S_{2b} crenulation cleavage carries a stretching lineation L_{52b} that plunges SSE, documenting a dominant dextral shearing component coupled with slight reverse motion (Figures 4d and 4e and 6).

The D_{2c} deformation corresponds to the last increment of D₂ with a progressive deformation along brittle reverse faults and an anastomosing network of regional brittle conjugate reverse shear zones (Figures 1b and 5f–5h). The NNE trending brittle reverse faults with a dip either to the west (N190°–41°W) near Sidi Bou Othmane, or to the east (N029°–53°E) elsewhere in the Jebilet massif, deform the dominant S_{2a} foliation (Figures 4f and 5f and 5g). Striated and polished planes with fibrous L_{R2c} mineral growth on reverse faults (Figures 4f and 5g) indicate top-to-the-west shearing in the Central Jebilet and top-to-the-east shearing in the Sidi Bou Othmane area (Figures 1b and 4f). The longest and the thickest strike-slip shear zones have a dominant trend at N244–84°NW (Mesret, Ait Bella shear zones) with reverse-dextral shearing, whereas those of the subsidiary set have a preferential trend at N306°–73°NE with reverse-sinistral shearing, generating sub-vertical F₃ kink folds (Figures 4f, 5h, 6, and 7f).

In summary, the Jebilet massif is characterized by a complex geometry resulting from two successive compressive events, D₁ and D₂. This polyphase deformation described in the Central Jebilet and in the west part of the Eastern Jebilet (Sidi Bou Othmane area) caused the formation of roughly E-W trending F₁ folds, superimposed by NNE- to NW trending F₂ folds resulting in type 2 fold interference patterns of Ramsay (1967) also called boomerang type (Figures 4b and 5a and 5c). This fold interference patterns exemplify a dual control of deformation by both the NNE and ESE oriented basement paleofaults (Aarab & Beauchamp, 1987; Bamoumen, 1988; Bamoumen et al., 2008; Huvelin, 1977) and changes in the regional crustal shortening direction over time. Nevertheless, in the east part of the Eastern Jebilet, this polyphase deformation is not noticeable as shown by folds trend disperse with a NE–SW mean orientation and variable vergence.

4. Geochronological Data

In order to define the age of magmatic events in the Variscan Jebilet massif, nine samples of granite intrusions corresponding to the granodiorites of Oulad-Ouaslam, Tabouchent and Bamega, and the acidic intrusion of Koudiat Hamra have been dated (Figure 1b).

4.1. Analytical Procedure and Material

U–Pb geochronological determination of zircon used LA-ICP-MS at BRGM, Orléans, France, with a quadrupole ICP-MS X series II coupled to a Cetac Excite 193 nm laser. Analyses were standardized with zircon 91500 (Wiedenbeck et al., 1995) and controlled with the Plešovice standard (338 ± 1 Ma, Sláma et al., 2008). Data reduction was done with GLITTER® software developed by Macquarie Research Ltd., and Concordia ages

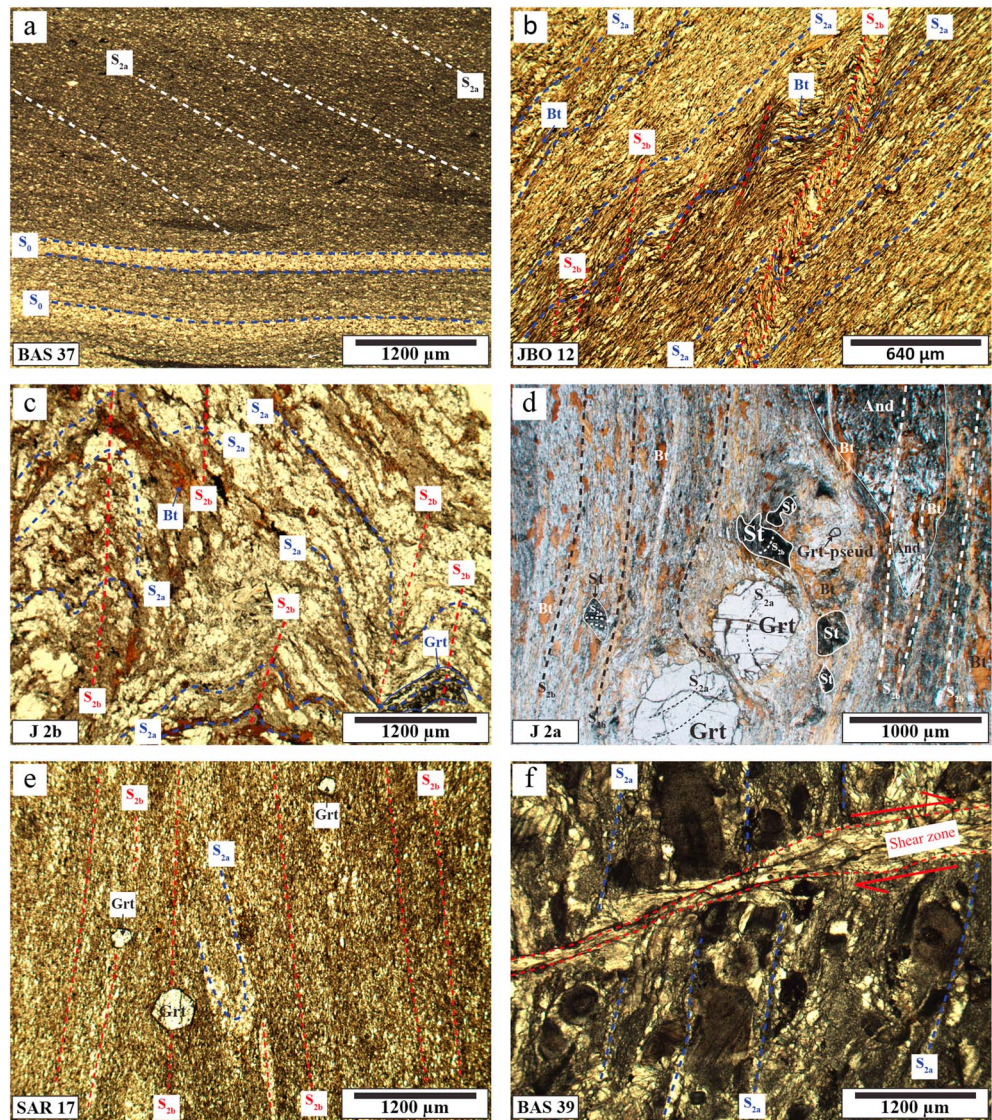


Figure 7. Microphotographs illustrating crystallization–deformation relationships. (a) S2 cleavage underlined by phyllosilicates crosscutting the bedding S0 in a greenschist-facies metapelitic sample of the Eastern Jebilet. (b and c) S2b crenulation cleavage refolding a S2a foliation developed respectively in a biotite micaschist and in a biotite-garnet micaschist. (d) Garnet and staurolite porphyroblasts with internal foliation S2a oriented at high angle to the main S2b foliation marked by elongated biotite and andalusite linked to syntectonic pluton emplacement. (e) Posttectonic garnets crosscutting the S2a and S2b foliation in the Sidi Bou Othmane area. (f) D2c shear zone crosscutting the main S2 foliation in a carbonate sample of the Teksim Formation.

and diagrams were generated using the Isoplot/Ex v.3 software package (Ludwig, 2003). Data acquired for samples JGO1, JGO3, JGO4, JTB1, JTB2, JTB3, and JTB4 were not corrected for common lead, and the proportions of ^{235}U were recalculated from the measured proportions of ^{206}Pb , ^{207}Pb , and ^{238}U and from the decay equations (Table S1). Data acquired for samples JGO2 and KH were corrected for common lead (Table S2); the correction was made using the $^{238}\text{U}/^{206}\text{U}$ and $^{207}\text{Pb}/^{206}\text{Pb}$ ratio measurements, following Tera and Wasserburg (1972) and Compston et al. (1992).

The analyzed zircons are morphologically homogeneous in all samples, with euhedral prismatic forms and an average long axis of $\sim 50\text{--}100\ \mu\text{m}$, with length-to-width ratios between 2:1 and 3:1. All zircons are transparent and colorless on cathodoluminescence images, made at BRGM using a TESCAN Mira 3 XMU MEB. They are either unzoned or more generally display a simple oscillatory zoning indicative of magmatic growth with rare old cores (Figure 8).

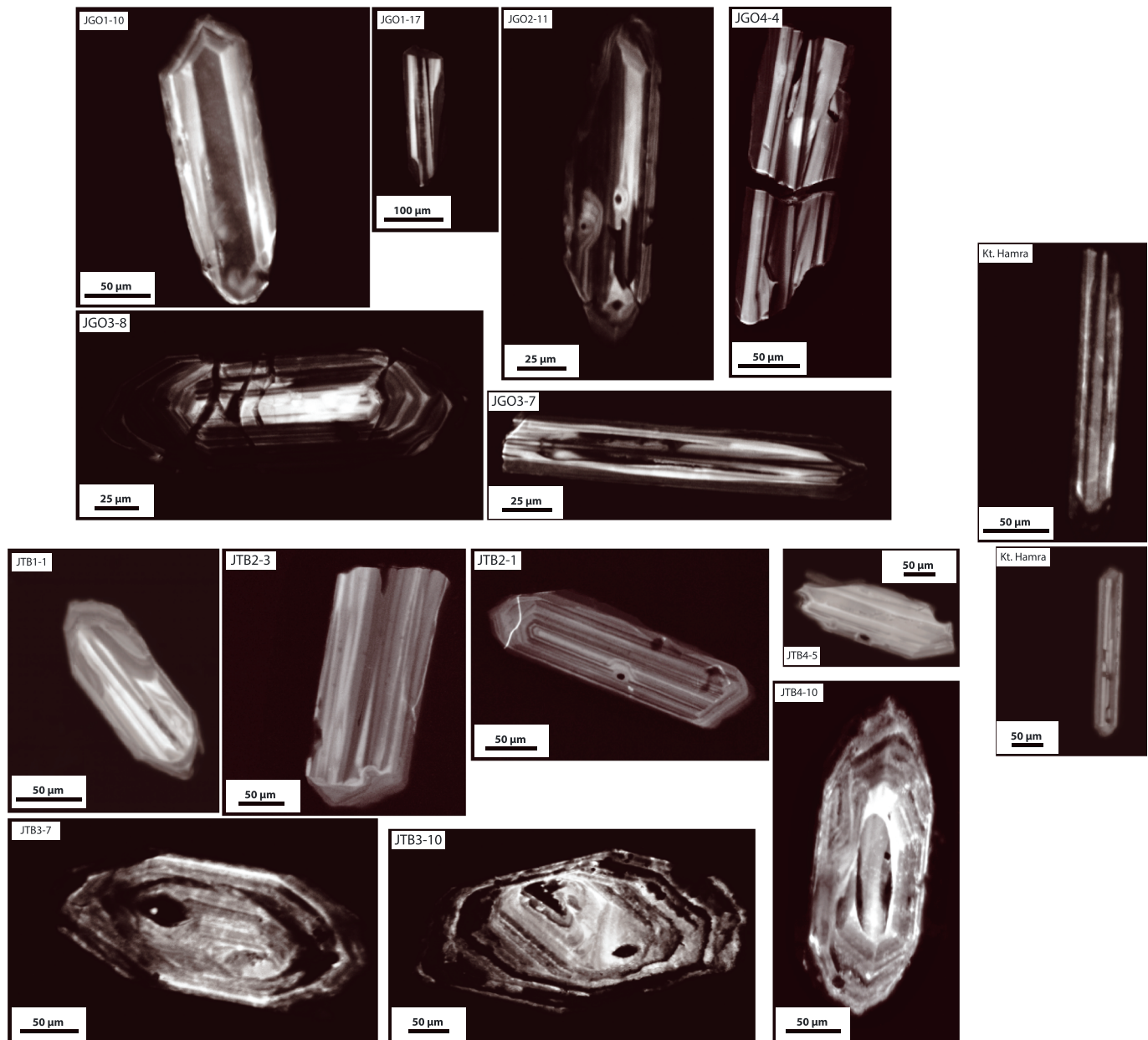


Figure 8. Cathodoluminescence images of representative zircons showing internal structures from the studied samples. JGO, Oulad-Ouslam granodioritic samples; JTB, Tabouchent-Bamega granodioritic samples; Kt. Hamra, Koudiat Hamra acidic pluton sample.

4.2. U-Pb Dating Results

Ouaslam Granodiorite. Four samples (JGO1, JGO2, JGO3, and JGO4) collected at different locations were dated on zircons (Figure 1b).

JGO1: of 61 analyses (Table S1), 4 show common lead ($^{204}\text{Pb} > 10$ cps [counts per second]) and 2 (JGO1-17 and JGO1-42) show significant disturbances of their U-Pb recordings (loss of lead and/or contamination). The concordant JGO1-52 and JGO1-23 analyses indicate ages of 700 and 470 Ma, respectively, and probably represent an inheritance (Figure 9a). The remaining 53 analyses are dispersed around 340 Ma. A further 11 analyses have $^{206}\text{Pb}/^{204}\text{Pb}$ ratios of < 500 and were disregarded in the age calculation. Among the remaining 42 analyses, 24 concordant to slightly discordant points yield an intercept at 337 ± 5 Ma (MSWD = 0.94). Some analyses seem to define an age of around 360 Ma, but the others would indicate loss of lead. The 337 ± 5 Ma age may correspond to the age of zircon crystallization, but, in any case, the dispersion of the analyses along

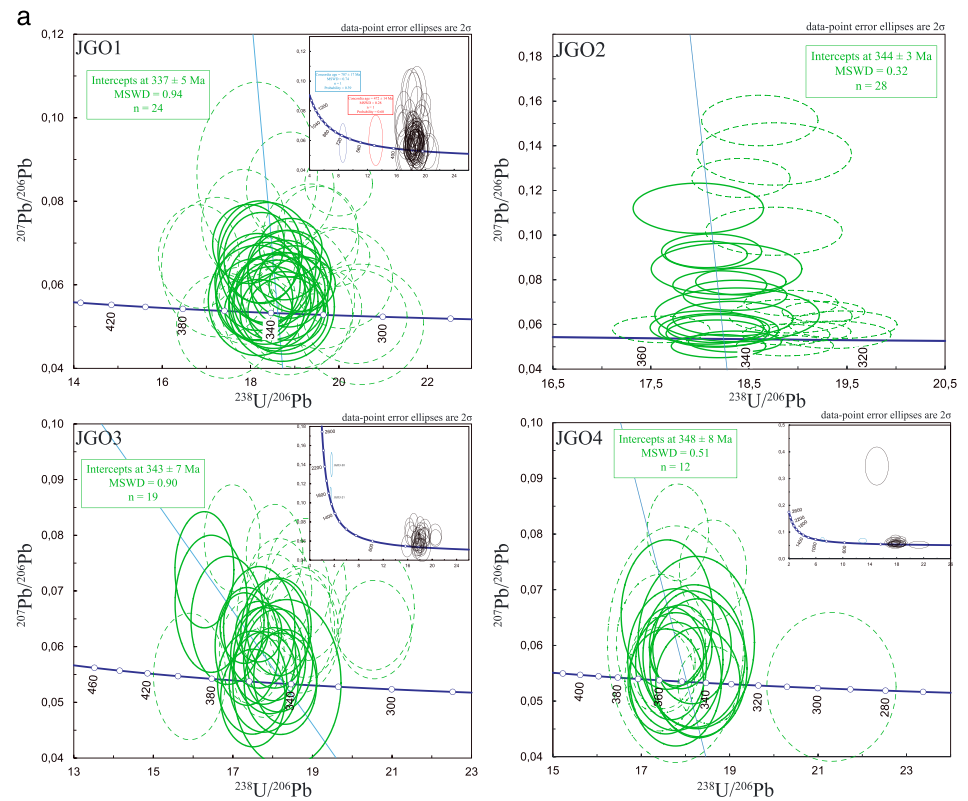


Figure 9. Concordia diagrams of laser ablation inductively coupled plasma-mass spectrometry (LA-ICP-MS) U-Pb zircon data from the studied samples. (a) Oulad-Ouaslami granodioritic samples. (b) Tabouchent-Bamega granodioritic samples. (c) Koudiat Hamra acidic sample. Data point error ellipses are 2σ ; MSWD, mean square of weighted deviation.

the Concordia between 360 and 310 Ma is a marker of major disturbance of the U-Pb system in this sample (inheritance, loss of lead, etc.).

JGO2: of 30 spots performed, old inheritance is obvious for one point (analysis-26; Table S2). The JGO-10 analysis is too contaminated in common lead to be used. The 28 remaining analyses scatter in age from 356 Ma (one point) to 345–325 Ma (considering concordant analyses). Fifteen concordant to slightly discordant points define a Discordia line with an intercept at 344 ± 3 Ma (MSWD = 0.32), interpreted as the crystallization age of the zircons during granite emplacement (Figure 9a), while the slightly younger ages from the other zircons could indicate a small loss of lead.

JGO3: 47 analyses were made (Figure 9a and Table S1). Of these, 12 show common lead ($^{204}\text{Pb} > 10$ cps) and are not plotted on the graphs and 2 (JGO3-21 and JGO3-30) indicate a Paleoproterozoic inheritance (Figure 9a). Among the 33 remaining analyses, 6 have $^{206}\text{Pb}/^{204}\text{Pb}$ ratios $< 1,000$ and were not considered and 19 concordant to slightly discordant points define a Discordia line with an intercept at 343 ± 7 Ma (MSWD = 0.90), seen as the zircon crystallization age. The other analyses probably represent a loss of lead.

JGO4: 27 analyses were carried out on single zircon crystals (Table S1). Among these, 4 show common lead ($^{204}\text{Pb} > 10$ cps) and 2 others (JGO4-7 and JGO4-8) indicate Precambrian ages, suggesting an old inheritance (Figure 9a). The JGO4-10 analysis is highly discordant, indicating a disturbance of the U-Pb system and thus disregarded. Of the 20 usable analyses, 12 concordant to slightly discordant points define a Discordia line with an intercept at 348 ± 8 Ma (MSWD = 0.51), interpreted as the probable age of crystallization. One remaining analysis (JGO4-27) is concordant and provides a $^{238}\text{U}/^{206}\text{Pb}$ mean age of 296 ± 8 Ma, interpreted as lead loss (Figure 9a).

Bamega and Tabouchent Granodiorites. Four samples (JTB1, JTB2, JTB3, and JTB4) collected at different locations were dated (Figure 1b).

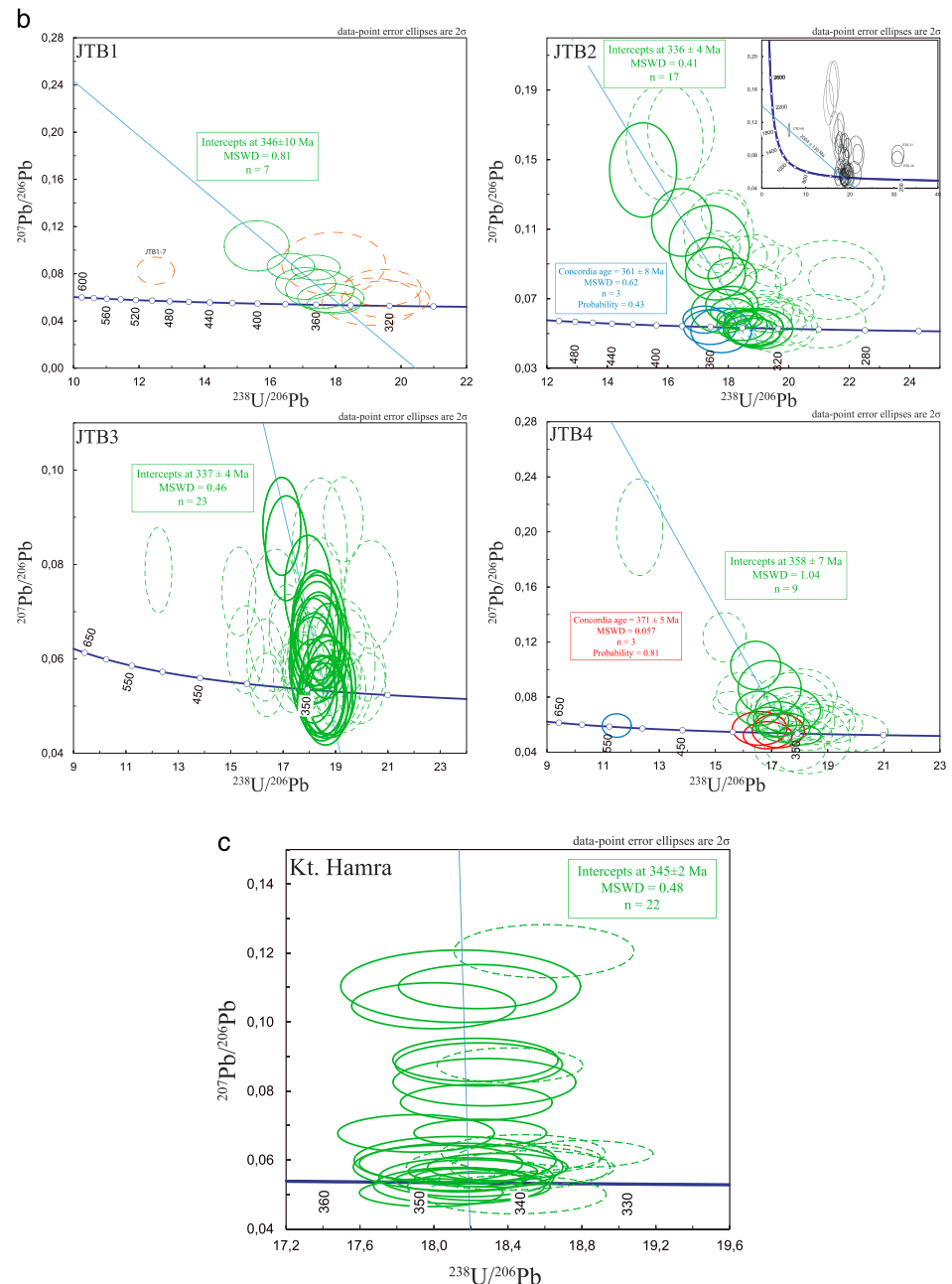


Figure 9. (continued)

JTB1: of the 19 analyses, 7 show common lead ($^{204}\text{Pb} \geq 10$ cps) and were not used for age calculation. The remaining 12 analyses were plotted on a Tera-Wasserburg diagram (Figure 9b). All results are listed in Table S1. Data obtained on spot JTB01-7 indicate ancient ages, likely reflecting the presence of an inherited core. Spots JTB01-18 and JTB01-19 show very low $^{206}\text{Pb}/^{204}\text{Pb}$ ratios (<300) and were not considered for the age calculation. Among the 9 remaining analyses, 7 concordant to slightly discordant points define a Discordia line with an intercept at 346 ± 10 Ma (MSWD = 0.81); the other 2 probably represent zircons with slight radiogenic lead losses.

JTB2: 60 analyses were realized, of which 14 show common lead ($^{204}\text{Pb} \geq 10$ cps) and were disregarded (Table S1). Analysis JTB02-60 indicates the presence of inherited lead, suggesting a Paleoproterozoic inheritance (Figure 9b). Analyses JTB02-21 and JTB02-26 show a strong loss of radiogenic lead combined with a

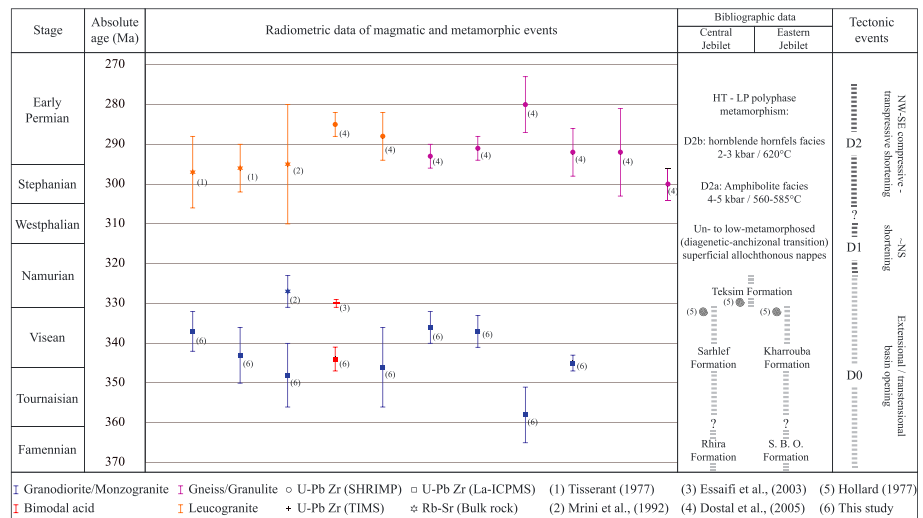


Figure 10. Interpretative temporal evolution of tectono-metamorphic events in the Jebilet massif from the Late Devonian to the Early Permian (see text for discussion).

significant contribution of common lead. The remaining 43 analyses were plotted on a Tera-Wasserburg diagram (Figure 9b). Of these, 12 have low $^{206}\text{Pb}/^{204}\text{Pb}$ ratios, <500 , and were disregarded; 3 concordant points located on the Concordia indicate slightly older ages than the other points at 361 ± 8 Ma (Figure 9b), and 17 concordant to slightly discordant points yield an intercept at 336 ± 4 Ma (MSWD = 0.41). Many analyses are located to the right of this discordia, which we interpret as being due to slight losses of lead (Pb^*).

JTB3: 53 spots were obtained (Table S1). Among them, 6 analyses show common lead ($^{204}\text{Pb} \geq 10$ cps and/or $^{206}\text{Pb}/^{204}\text{Pb} < 500$) and were disregarded. Another 23 analyses are concordant or slightly discordant and define a Discordia line with a weighted $^{238}\text{U}/^{206}\text{Pb}$ mean age of 337 ± 4 Ma (MSWD = 0.46), interpreted as the probable age of crystallization (Figure 9b). Some analyses seem to define an even earlier age around 350 Ma, but their number is below the analytical density, which results in an age of 337 Ma. Other analyses to the right of the Discordia are interpreted as being affected by loss of Pb^* .

JTB4: 38 spots were obtained on single zircon crystals (Figure 9b), 6 of which present common lead ($^{204}\text{Pb} \geq 10$ cps) and are not shown on the U-Pb graph (Figure 9b). All analyses are shown in Table S1. Among them, the JTB04-12 analysis is concordant at about 540 Ma and probably represents an inherited core. The remaining 31 are widely dispersed with ages ranging from 320 to 370 Ma. Many analyses have low $^{206}\text{Pb}/^{204}\text{Pb}$ ratios (<500) and were disregarded, 3 analyses are concordant at 371 Ma (Figure 9b), and 9 others allow drawing a discordia whose intercept gives an age of 358 ± 7 Ma (MSWD = 1.04). The other analyses indicate loss of radiogenic lead. This discordia remains questionable through the dispersion of the analytical points but can represent the crystallization age of these zircons with a slightly older inheritance.

Koudiat Hamra Acidic Pluton. One sample (KH) was collected to date the bimodal acidic pluton in the Central Jebilet (Figure 1b), and 30 spots were made on sample Kt. Hamra (Table S2). Among them, 22 analyses define a Discordia line with a weighted $^{238}\text{U}/^{206}\text{Pb}$ mean age of 345 ± 2 Ma (MSWD = 0.48; Figure 9c); the remaining 8 analyses are interpreted as being affected by lead loss.

5. Discussion

5.1. Late Paleozoic Magmatic and Tectono-metamorphic Evolution of the Jebilet Massif

The combination of our new structural observations and U/Pb age determinations allows us to better constrain the magmatic, metamorphic, and tectonic evolution of the Jebilet massif from the Famennian-Late Viséan/Namurian preorogenic stage (370–325 Ma) to the Westphalian-Permian compressional stage (325–270 Ma). This geological evolution of the Jebilet massif is summarized in Figures 10 and 11.

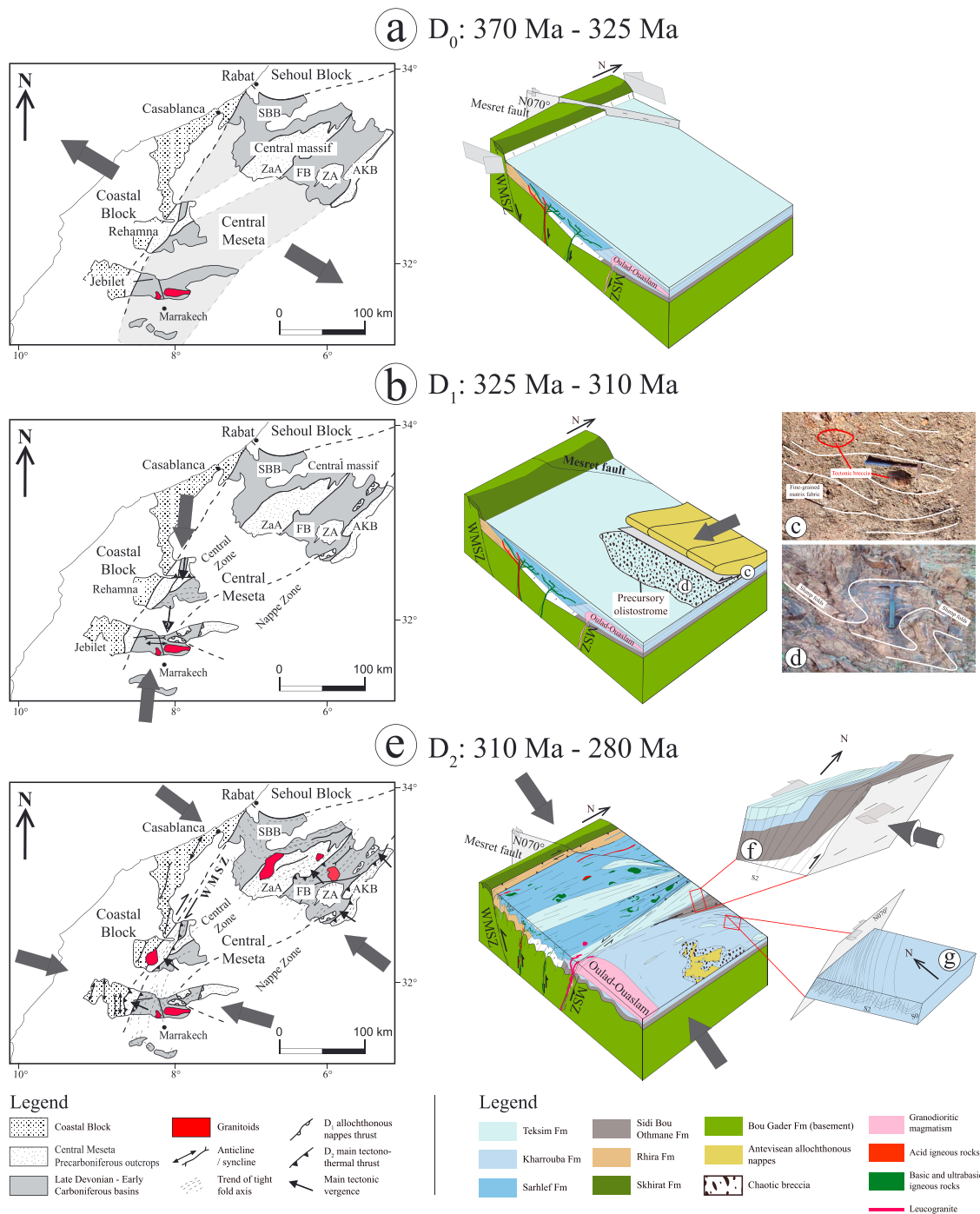


Figure 11. Maps (modified after Michard et al., 2010; Wernert et al., 2016) and three-dimensional idealized model for the evolution of the Moroccan Meseta domain and the Jebilet Massif from the Late Devonian to the Early Permian (see text for discussion). The large gray arrows correspond to the crustal shortening direction. Za, Zaian anticlinorium; ZaA, Zaer anticlinorium; FB, Fourhal basin; AKB, Azrou-Khenifra basin; SBB, Sidi Bettache basin.

5.1.1. Famennian to Visean-Namurian (370–325 Ma): Opening of the Jebilet Intracontinental Basin and Magmatism

Stratigraphic studies have shown that the Jebilet massif was an area of marine sedimentation from Late Devonian to Early Carboniferous, linked to the opening of an intracontinental basin (Figures 10 and 11a). Sedimentation started with the deposit of the Famennian (370 Ma) Rhira Formation and finished with the Late Visean-Namurian (325 Ma) Teksim Formation (Aarab & Beauchamp, 1987; Beauchamp, 1984;

Bordonaro, 1983; Hollard et al., 1977; Huvelin, 1977; Izart et al., 1997; Mayol, 1987). As proposed by Aarab and Beauchamp (1987), the opening (D_0) of the Jebilet basin was controlled by $\sim N70$ sinistral transcurrent faults associated with $\sim N20$ normal faults that developed a transtensional pull-apart basin (Figure 11a).

Geochemical studies on the bimodal magmatism of the Central Jebilet confirmed the extensional tectonic regime during this period. Bordonaro (1983), Aarab (1984, 1995), and Aarab and Beauchamp (1987) demonstrated that the cogenetic bimodal association of tholeiitic mafic/ultramafic intrusive rocks and calc-alkaline felsic intrusive rocks, resulted from the differentiation of a tholeiitic magma, emplaced in an intracontinental rift during the preorogenic phase. These observations were confirmed by Bamoumen et al. (2008) in the Eastern Jebilet, where trace element compositions of basaltic and trachytic rocks show an alkaline and a tholeiitic signature in the field of intraplate anorogenic basalt. This transtensional setting is also accredited by (1) the abundant volcanism hosting massive sulfides, dated at 331.7 ± 7.9 Ma (Marcoux et al., 2008) and emplaced at the top of the Sarhlef Formation dated Late Visean (Asbien, Moreno et al., 2008; Playford et al., 2008), and (2) the sedimentation of the Teksim Formation (Figure 10).

The protholitic ages of 345 ± 2 Ma and 358–336 Ma obtained in this study for the Kt. Hamra bimodal acid intrusion and for the Oulad-Ouaslam and Tabouchent/Bamega granodiorites, respectively (Figure 10), coincide with this period of transtensional basin opening (Figure 11a). We assume a similar age for the other acid intrusions (Kt. Bouzlaf and Kt. Diab) and the mafic intrusions considered as cogenetic (bimodal association; Essaifi et al., 2013).

As shown in Figure 10, these new radiometric ages are much older than the previous ones proposed by Mrini et al. (1992) for the Oulad-Ouaslam intrusion at 327 ± 4 Ma (Rb-Sr dating on whole rock) and by Essaifi et al. (2003) for bimodal acidic intrusions at 330.5 ± 0.68 – 0.83 Ma (ID-TIMS U-Pb on zircon, reverse discordia, one concordant point), which significantly modifies the tectono-thermal interpretation of the Jebilet massif. Indeed, since the structural work of Lagarde and Choukroune (1982), Le Corre and Saquaque (1987), and Essaifi et al. (2003)—all considering these intrusions as approximately 330 Ma-old, syntectonic and emplaced during a transpressional regime—the main tectono-thermal event in the Jebilet massif was considered to have been Late Visean (~ 330 Ma). However, the crystallization ages of ~ 330 Ma estimated for the Oulad-Ouaslam and the bimodal acidic intrusions are hardly compatible with the Late Visean stratigraphic age (~ 330 Ma) attributed to the top of Kharrouba and Sarhlef formations in which these intrusions were emplaced (Figures 10 and 11a). Therefore, the ages of Mrini et al. (1992) and Essaifi et al. (2003) can date neither the crystallization of both Oulad-Ouaslam granodiorite and acidic intrusions nor the main *compressive* tectono-thermal event in the Jebilet. This interpretation is supported by the work of Boummane and Olivier (2007), which, by combining anisotropy of magnetic susceptibility technique and microstructural studies, shows that the complete crystallization of the Oulad-Ouaslam intrusion predated the Variscan shortening. This conclusion can be extended to the Bamega-Tabouchent intrusions dated by us at 355 Ma and where similar structures of deformation were described by Le Corre and Saquaque (1987).

Considering our geochronological data, we conclude that the Jebilet massif, located in the external part of the Variscan orogen, represents an intracontinental basin that underwent an extensional/transensional tectonic regime from the Famennian (370 Ma) to the Late Visean-Namurian (325 Ma). This crustal opening was accompanied by major granodioritic and bimodal magmatism emplaced in deepwater-marine sedimentary rocks on a thinned continental crust.

5.1.2. Late Carboniferous to Early Permian (325–270 Ma): Variscan Deformation of the Jebilet

In the Jebilet massif, the first expression of the Variscan compression corresponds to the formation of D_1 recumbent folds related to the emplacement of superficial allochthonous nappes (Figures 10 and 11b). Our structural analysis emphasized the presence of a tectonic breccia (tectonic mélange) related to thrust faulting (Figure 11c), subhorizontal boudins, and the absence of regional-scale S_1 cleavage. At the map scale (Figure 1b), the tectonic mélange defines a narrow zone (a few dozen meters) in the footwall of the allochthonous superficial nappes. However, away from the thrust faults, our field observations show that the chaotic breccia is characterized by slump folds affecting the sediments (Figure 11d). This kind of deformation commonly occurred in poorly lithified material and represents soft-sediment deformation related to slope instabilities at very shallow structural levels. In the same area, Huvelin (1977) described the presence of an olistostrome composed of reworked flysch associated with a sedimentary mélange formed by numerous native and exotic olistoliths, respectively from the Kharrouba Formation and the allochthonous nappes;

this author attributed the olistostrome as a product of mass-transport deposits. Moreover, we interpret that superficial nappes were emplaced in a compressive regime (Graham, 1982a; Zahraoui, 1981) and must not be attributed to a synsedimentary gravitational process as proposed by Bamoumen et al. (2008), Beauchamp and Izart (1987), and Huvelin (1977).

The Jebilet massif is characterized by sedimentary mélanges (Figures 11b and 11d) overprinted by tectonic deformation in the footwall of a thrust related to allochthonous nappe emplacement (Figures 11b and 11c). The interplay between sedimentary and tectonic mélanges, and the superposition of these different processes resulting in a polygenetic mélange, are typical of compressional deformation settings (Festa et al., 2010, 2012, 2016). The D_1 compressive deformation caused the emplacement of a precursory olistostrome, composed of a sedimentary mélange generated by gravity sliding at the active front of the allochthonous superficial nappes, which was then overridden by these nappes and incorporated into the thrust faults reworking the sedimentary mélange into a tectonic mélange (Figures 11b–11d).

The tectonic transport of D_1 allochthonous superficial nappes is difficult to decipher, due to scarce kinematic indicators and strong overprinting by D_2 deformation, which induced a major dispersion of D_1 structures from N000 to N090 in the east of the Eastern Jebilet. Considering that this area is attached to the Nappe Zone of the Meseta Domain, a NW directed kinematics is admitted (Hoepffner et al., 2005; Michard et al., 2010). Nevertheless, in the Central Jebilet and the western part of the Eastern Jebilet (Sidi Bou Othmane area), our structural analysis shows for the first time the presence of roughly E-W trending F_1 folds, suggesting ~N-S shortening whose vergence is unknown. Considering the south vergent thrusting proposed by Chopin et al. (2014) in the Rehamna (see section 5.2, hereafter), a top to the south vergence could be proposed for D_1 (Figure 11b). The south vergence proposed should be taken with caution, as no direct field evidence has been observed in the Jebilet massif. This contrast between dispersive D_1 structures in the east of the Eastern Jebilet, and the well-ordered D_1 structures trending roughly E-W in the Central Jebilet and the west of the Eastern Jebilet, could represent a D_1 deformation recorded at different structural levels (Figure 11b). In the eastern Jebilet, mineralogical and RSCM geothermometry studies in the Kharrouba Formation show a Chl-Phg-Qtz-Ab paragenesis (Huvelin, 1977) and RSCM temperatures estimated around 350 °C (Delchini et al., 2016), indicating both conditions of greenschist facies metamorphism. However, microstructural analyses clearly show that mineral growths are associated with the S_{2a} slaty cleavage (Figure 7a), demonstrating that peak metamorphism in the Jebilet massif postdates D_1 and correlates with the dominant D_2 deformation. Thus, D_1 allochthonous nappes were superficial, emplaced under very low metamorphic conditions (150–200 °C; Bamoumen, 1988). These results show that D_1 recumbent folding and thrusting did not generate stacking and crustal thickening, nor contribute to metamorphism. The age of the D_1 compressional event is constrained by the biostratigraphic age of the youngest sediments of the Late Visean-Namurian Teksim Formation: the initiation of the Variscan D_1 compressional event causing nappe emplacement thus postdates the Visean-Namurian (~325 Ma; Figures 10 and 11b).

The second stage of Variscan compression (D_2 , Figure 11e) started with the development of large-scale isoclinal F_{2a} folds accompanied by a S_{2a} axial foliation, dominated by a strong planar fabric indicating bulk coaxial deformation by flattening (S-type tectonites). When D_2 deformation increased, a N020 reverse-dextral shear component became dominant, corresponding to the transpressional D_{2b} phase (Figure 11f). These structures are intersected, or reoriented, by D_{2c} deformation, which corresponds to the last increment of D_2 (Figure 11g). D_{2c} is characterized reverse faults and an anastomosing network of regional brittle conjugate reverse shear zones.

The D_2 deformation reveals a progressive evolution from bulk contractional coaxial deformation to noncoaxial dextral transpression, consistent with WNW-ESE to NW-SE horizontal shortening (Figure 11e) and can be described as a continuous deformation leading to an asymmetric positive flower structure (Bordonaro, 1983; Essaifi et al., 2001; Lagarde, 1985; Lagarde & Choukroune, 1982; Le Corre & Bouloton, 1987), inducing a moderate crustal thickening.

The development of the penetrative subvertical cleavage associated with D_{2a} was accompanied by an M_{2a} regional metamorphism in the greenschist facies (Figure 7a), in the Central and Eastern Jebilet; only in the Sidi Bou Othmane area a garnet-staurolite association was described indicating amphibolites facies metamorphic conditions (Grt and St, Figure 7d). Thermobarometric and RSCM geothermometry studies give an

HT-LP metamorphic peak of 4 to 5 kbar and 560–585 °C for the M_{2a} regional metamorphism (Delchini et al., 2016).

In most of the Central and Eastern Jebilet, D_{2b} transpression occurred under low-grade regional retromorphic metamorphism (Figures 7b and 7c) and was accompanied by the emplacement of syntectonic to posttectonic leucogranitic intrusions, such as the Bramram pluton. The latter induced an HT-LP M_{2b} contact metamorphism reaching the hornblende-hornfels facies (Delchini et al., 2016; El Hassani, 1980). Some of these intrusions are considered hidden at shallow depth, in particular in the Sidi Bou Othmane area (Figure 1b), where they are only suspected by their contact metamorphism characterized by syntectonic to posttectonic mineralogical assemblages (And-Grt-Bt in metapelite; Figures 7d and 7e). Quantitative pressure and temperature conditions estimated by Raman geothermometer and thermobarometric calculations are in agreement with the paragenetic observations and give peak conditions of 2–3 kbar and 620 °C (Delchini et al., 2016).

The timing of the D_2 deformation is not directly dated. However, field observations indicate that leucogranitic dykes and stocks (Bramram), dated at 297 ± 9 Ma, 296 ± 6 Ma (Tisserant, 1977) and 295 ± 15 Ma (Mrini et al., 1992), were syntectonic to postkinematic with respect to D_{2b} deformation (Figures 10 and 11e). These ages were confirmed by the SHRIMP U-Th-Pb radiometric study by Dostal et al. (2005) on zircons in igneous xenoliths (leucogranite, gneiss, and granulite) within lamprophyric dykes. Leucogranite xenoliths gave ages at 285 ± 3 and 288 ± 6 Ma, agreeing with previous age determinations by Tisserant (1977) and Mrini et al. (1992), considering the analytical uncertainties (Figure 10). Dating of metamorphic rims on zircon grains from gneiss and granulite yielded ages of 280 ± 7 Ma, 292 ± 6 Ma, 292 ± 11 Ma, and 300 ± 4 Ma, which given the mineral parageneses Qtz-Fsp-Grt-Sill-Ky and Qtz-Fsp-Bt-Grt (Dostal et al., 2005) can be interpreted as the ages of the M_{2a} peak metamorphism. Ages attributed to D_{2a} and D_{2b} deformation are similar, considering the analytical uncertainties. Therefore, we propose an age ranging between 310 and 280 Ma for the D_2 episode (Figures 10 and 11e).

The D_2 HT-LP metamorphism recorded in the Jebilet massif cannot be explained by crustal thickening. Moderate thickening associated to HT-LP metamorphism (Figure 11e) can be explained by an inherited HT thermal anomaly, developed during the Late Devonian-Early Carboniferous intracontinental rifting as proposed in the Rehamna and Jebilet massifs by Michard et al. (2010), and for the Rehamna by Wernert et al. (2016). In the case of the Jebilet massif, we therefore propose that the HT thermal anomaly related to the D_0 rifting episode was responsible for the bimodal and granodioritic magmatism around 340 Ma (Figure 10) and induced a thermal softening of the crust. Then, as demonstrated by the thermomechanical models of Thompson et al. (2001), the inversion of this thermally weakened intracontinental domain during the Variscan compression (D_1 , D_2) around 310 Ma (Figure 10) caused moderate crustal thickening and HT-LP metamorphism associated to leucogranitic magmatism. The models of Schulmann et al. (2002) and Thompson et al. (2001) showed that heat input during continental rifting can be still active up to 30–40 Ma after cessation of the thermal anomaly, influencing the thermomechanical properties of the crust.

5.2. Regional Implications

The geological evolution of the Jebilet massif from Late Devonian to Early Permian as proposed in this study provides valuable results for better understanding the MMD geological history.

The extensional/transensional D_0 tectonics of the Jebilet massif from Late Devonian to Visean-Namurian times is consistent with the opening of Devonian-Carboniferous basins in the paleo Western Meseta (Figure 11a), controlled by pull-apart tectonics (Aarab & Beauchamp, 1987; Bouabdelli & Piqué, 1996; Piqué & Michard, 1989). By contrast, our results are opposed to the model proposed by Ben Abbou et al. (2001) and Roddaz et al. (2002) in the Nappe Zone, extended to the Jebilet massif by (Essaifi et al., 2001, 2003, 2013), who considered these basins as back-arc foreland basins related to north-westward propagation of a thrust-and-fold belt originating in the Eastern Meseta. Intracontinental rifting was associated with major bimodal and granodioritic magmatism dated in the Jebilet massif at 358–336 Ma. Similar ages have been obtained on bimodal intrusions in the Western Meseta (ranging between 349 and 339 Ma; Ait Lahna et al., 2018). As shown by Chopin et al. (2014) and Wernert et al. (2016) in the Rehamna massif and by us in the Jebilet, this important magmatism testifies to an active thermal anomaly throughout this area, probably caused by mantle heat advection.

Our interpretation is reinforced by the observation that the whole northern Gondwana margin, from North Africa to Arabia, underwent a Late Devonian to Early Carboniferous rifting event (Frizon de Lamotte et al., 2013), characterized by general subsidence, deposition of sediments, and emplacement of magma. This dynamic is attributed to a large-scale clockwise rotation of Gondwana related to the opening of the Paleotethys Ocean associated to a large-scale mantle anomaly (Edel et al., 2018; Frizon de Lamotte et al., 2013). In fact, high heat flow, magmatism, and HT-LP metamorphism event at approximately 340 Ma, caused by mantle heat advection and related to Paleotethys rifting, affected different areas across the entire Variscan belt as shown by Franke (2014) and Franke et al. (2017).

The tectonic inversion of the Jebilet basin is recorded at Viséan/Namurian (325 Ma). The earliest D_1 compressive event was characterized by the emplacement of superficial nappes. This deformation can be correlated with the folds, duplexes, and nappe structures developed sequentially from east to west (top to the NW-WNW) in the Nappe Zone and the Fourhal Basin of the Central Massif (Figure 1a; Ben Abbou et al., 2001; Bouabdelli, 1994; Roddaz et al., 2002). The D_1 event in the Jebilet could also correspond to the D_1 folds and thrusts described from the low-metamorphosed to unmetamorphosed units of the Rehamna massif, whose vergence is considered either top to the W-NW (Aghzer & Arenas, 1995, 1998; Baudin et al., 2003), or top to the SW-SSW (Chopin et al., 2014; Corsini et al., 1988).

We show that in the Central Jebilet and the west part of Eastern Jebilet, the well-ordered D_1 folds trending roughly E-W are compatible with a N-S crustal shortening, as proposed by Chopin et al. (2014) in the Rehamna massif for D_1 deformation and related to a top to SSW thrusting. Therefore, a similar kinematic could be supposed for the Jebilet nappes (Figure 11b).

Nevertheless, in the east of the Eastern Jebilet, the various kinematics (top to the west, top to the south, top to the south-east, top to the north-west, and top to the north) proposed by Huvelin (1977), Bamoumen (1988), and Zahraoui (1981) show that the vergence of the D_1 event was poorly understood. In this area, the strong dispersion of D_1 structures and kinematic indicators related to overprinting by D_2 deformation does not allow us to propose a kinematic for emplacement of superficial nappes. Considering that the east part of Eastern Jebilet is classically attached to the Nappe Zone, which runs NE-SW along all the other MMD (Figure 11b), a NW directed kinematics cannot be excluded (Hoepffner et al., 2005; Michard et al., 2010).

Regardless of kinematics directions, we show that the earlier emplacement of superficial D_1 nappes in the Jebilet massif did not generate stacking and crustal thickening nor did it contribute to metamorphism. Therefore, this emplacement cannot be correlated to the D_1 event as proposed by Aghzer and Arenas (1995, 1998) and Baudin et al. (2003) for the Rehamna massif, where the barrovian metamorphism is ascribed to tectonic nappe stacking. Similarly, Chopin et al. (2014) and Wernert et al. (2016) also attributed the barrovian metamorphism—affecting the lower metamorphic unit of the Rehamna massif—to the D_1 event dated between 310 and 300 Ma, and corresponding to the peak of pressure (Chopin et al., 2014; Wernert et al., 2016). Nevertheless, these authors considered that this D_1 barrovian metamorphism was generated by an inherited postrift thermal anomaly associated to moderate crustal thickening, inducing horizontal ductile flow in the infrastructure. In this scheme, the emplacement of superficial D_1 nappes at high structural levels in the Jebilet may be assimilated to deformation affecting the superstructure. This interpretation could explain the contrasting deformation between the infrastructural lower metamorphic unit of the Rehamna—recording the pressure peak—and the superstructural low-metamorphosed to unmetamorphosed succession exposed in the Jebilet massif.

In the Fourhal basin, located farther north in the Central Massif (Figure 1a), turbiditic sedimentation into D_1 N-NW verging flexural folds persisted from the Namurian until the Early Westphalian (~315 Ma). This age of around 315 Ma seems the best estimate for the end of marine sedimentation in the MMD and can therefore be considered as the transitional age between the D_1 and D_2 events.

The main D_2 Variscan phase in the Jebilet massif, characterized by NNE trending folds with a dextral shearing component and associated HT-LP metamorphism, is dated as Late Pennsylvanian-Early Permian (310–280 Ma; Figure 10). Similar deformation is well known elsewhere in MMD; in the Massif Central, for instance, Late Pennsylvanian-Early Permian structures are characterized by NNE to NE trending folds with a NW or SE kinematic, followed by ductile-brittle reverse faults and strike-slip shear zones (Figure 11e). The

Rehamna massif was also affected by NW-SE to WNW-ESE crustal shortening that followed the exhumation of the lower metamorphic unit (Figure 11e; Baudin et al., 2003; Chopin et al., 2014). The latter event is associated with HT-LP metamorphism and syntectonic to posttectonic magmatism dated between 292 and 275 Ma (Chopin et al., 2014), with a thermal peak age at ~ 276 Ma (Wernert et al., 2016). At the scale of the MMD, the NW-SE to WNW-ESE compressive episode was related to dextral transpression along the WMSZ (Hoepffner et al., 2006, 2005; Michard et al., 2010; Piqué et al., 1980). Michard et al. (2010) suggested that HT-LP metamorphism accompanying this compressive event in the Rehamna and the Jebilet was controlled by an older thermal anomaly in relation with the Late Devonian-Early Carboniferous intracontinental rifting stage. This hypothesis is also supported by Chopin et al. (2014) and Wernert et al. (2016) for the Rehamna massif. Our results have further confirmed this model for the Jebilet massif.

At a plate dynamics scale, the D_2 event in the MMD coincided either with the final closure of the Rheic Ocean (Nance et al., 2010, 2012) or with the closure of the Paleotethys Ocean (Edel et al., 2018) depending of the scenario, through a general clockwise rotation of Gondwana relative to Laurussia. This took place from the Late Carboniferous to the Early Permian and resulted in the Alleghanian-Variscan orogeny (Chopin et al., 2014; Edel et al., 2018; Frizon de Lamotte et al., 2013; Hatcher, 2002, 2010; Kroner et al., 2016).

6. Conclusions

From Late Devonian to Early Carboniferous, the Jebilet basin opened as shown by sedimentary infill and by abundant traces of magmatic activity, dated in this study between 358 ± 7 Ma and 336 ± 4 Ma. These ages are older than those previously proposed by Mrini et al. (1992) and Essaifi et al. (2003) and demonstrate that the magmatism of the Jebilet was emplaced *before* the shortening episodes as already proposed by Bordonaro (1983), Aarab (1984), and Aarab and Beauchamp (1987).

The structural shape of the Jebilet massif results from the superposition of two deformation events, D_1 and D_2 from Late Carboniferous to Early Permian:

1. D_1 corresponds to the emplacement of superficial nappes at high structural level resulting in NS shortening in the Central Jebilet and in the west part of the Eastern Jebilet, and whose vergence could be top to the SSW by correlation with the Rehamna massif. Nevertheless, in the east part of the Eastern Jebilet, no clear kinematic could be identified. Considering that this part is classically attached to the Nappe Zone, which runs NE-SW along all the other MMD, a NW directed kinematics cannot be excluded.
2. D_2 corresponds to a continuous deformation event involving westward thrusting onto the Coastal Block via the WMSZ. This induced major NW-SE transpressional crustal shortening was accompanied by HT-LP metamorphism. The absence of crustal stacking in the Jebilet massif seems to indicate that the high-T metamorphic event and associate magmatism are related to the inherited post-rift thermal anomaly, as proposed for the Rehamna and Jebilet massifs by Michard et al. (2010) and for the Rehamna by Chopin et al. (2014) and Wernert et al. (2016).

The complex evolution of the Jebilet massif from the Late Devonian to the Early Permian can be regarded as a result of large-scale thermal and mechanical processes related to the reorganization of Gondwana and Laurussia megaplates and opening of the Paleotethys generating a mantle anomaly as proposed by Simancas et al. (2009) and Frizon de Lamotte et al. (2013).

Acknowledgments

This work was conducted thanks to the French Geological Survey (BRGM, Orléans, France) and the ISTO laboratory (Orléans, France), both of whom provided financial support for fieldwork and analysis. We thank the Editor M. Jolivet, the Associate Editor, the two anonymous reviewers, and M. Corsini for their suggestions that improved the version of this manuscript. H. M. Kluijver edited the English version of the manuscript. Supporting data are included in supporting information or available by contacting the corresponding author (s.delchini@brgm.fr).

References

- Aarab, E. M. (1984). Mise en évidence du caractère co-génétique des roches magmatiques basiques et acides dans la série volcano-sédimentaire de Sarhlef (Jebilet, Maroc Hercynien). Univ. Nancy I.
- Aarab, E. M. (1995). Genèse et différenciation d'un magma tholéïitique en domaine extensif intracontinental: exemple du magmatisme pré-orogénique des Jebilet (Maroc hercynien), (Thèse de 3ème Cycle). Marrakech: Univ. Cadi Ayad.
- Aarab, E. M., & Beauchamp, J. (1987). Le magmatisme carbonifère pré-orogénique des Jebilet centrales (Maroc). Précisions pétrographiques et sédimentaires. Implications géodynamiques. *Comptes Rendus. Académie des Sciences*, 304, 169–174.
- Aghzler, A. M., & Arenas, R. (1995). Detachments and extensive tectonics in the hercynian Rehamna massif (Morocco). *Journal of African Earth Sciences*, 21(3), 383–393. [https://doi.org/10.1016/0899-5362\(95\)00096-C](https://doi.org/10.1016/0899-5362(95)00096-C)
- Aghzler, A. M., & Arenas, R. (1998). Metamorphic evolution of the metapelites of the Hercynian Massif in Rehamna (Morocco): Tectonothermal implications. *Journal of African Earth Sciences*, 27(1), 87–106. [https://doi.org/10.1016/S0899-5362\(98\)00048-7](https://doi.org/10.1016/S0899-5362(98)00048-7)
- Ait Lahna, A., Aarab, E. M., Nasrddine, Y., Colombo Celso Gaeata, T., Bensalah, M., Boumechdi, M. A., et al. (2018). The Lalla Tittaf Formation (Rehamna, Morocco): Paleoproterozoic or Paleozoic age?

- Bamoumen, H. (1988). Géométrie et cinématique de la déformation dans les nappes hercyniennes des Jebilet centre-orientales, Maroc, (Thèse de 3ème Cycle). Univ. de Marrakech.
- Bamoumen, H., Aarab, E. M., & Soulaïmani, A. (2008). Tectono-sedimentary and magmatic evolution of the Upper Visean basins of Azrou-Khénifra and eastern Jebilet (Moroccan Meseta). *Estudios Geológicos*, 64(2), 107–122.
- Baudin, T., Chèvremont, P., Razin, P., Youbi, N., Andries, D., Hoepffner, C., & Tegye, M. (2003). Carte géologique du Maroc au 1/50 000, feuille de Skhour des Rehamna, Mémoire explicatif. *Notes et Mémoires du Service Géologique du Maroc*, 435, 1–114.
- Beauchamp, J. (1984). Le Carbonifère inférieur des Jebilet et de l'Atlas de Marrakech (Maroc); migration et comblement d'un bassin marin. *Bulletin de La Société Géologique de France*, 7(6), 1025–1032.
- Beauchamp, J., & Izart, A. (1987). Early Carboniferous basins of the Atlas-Meseta domain (Morocco); sedimentary model and geodynamic evolution. *Geology*, 15(9), 797–800. [https://doi.org/10.1130/0091-7613\(1987\)15<797:ECBOTA>2.0.CO;2](https://doi.org/10.1130/0091-7613(1987)15<797:ECBOTA>2.0.CO;2)
- Belkabar, A., Gibson, H. L., Marcoux, E., Lentz, D., & Rziki, S. (2008). Geology and wall rock alteration at the Hercynian Draa Sfar Zn-Pb-Cu massive sulphide deposit, Morocco. *Ore Geology Reviews*, 33(3–4), 280–306. <https://doi.org/10.1016/j.oregeorev.2007.03.001>
- Ben Abbou, M., Soula, J. C., Brusset, S., Roddaz, M., N'Tarmouchant, A., Driouch, Y., et al. (2001). Contrôle tectonique de la sédimentation dans le système de bassins d'avant-pays de la Meseta marocaine. *Comptes Rendus de l'Académie Des Sciences de Paris*, 332, 703–709.
- Bensalah, M. K. (1989). Etude pétrographique, géochimique et structurale des massifs granitiques de Baméga-Tabouchent-Brambram et Ouled Ouaslam (Jebilet, Maroc), (Thèse 3ème Cycle). Univ. Marrakech.
- Bernard, A. J., Maier, O. W., & Mellal, A. (1988). Aperçu sur les amas sulfurés massifs des Hercynides marocaines. *Mineralium Deposita*, 23(2), 104–114.
- Bernardin, C., Cornée, J. J., Corsini, M., Mayol, S., Muller, J., & Tayebi, M. (1988). Variations d'épaisseur du Cambrien moyen en Meseta marocaine occidentale: signification géodynamique des données de surface et de subsurface. *Canadian Journal of Earth Sciences*, 25(12), 2104–2117. <https://doi.org/10.1139/e88-194>
- Bordonaro, M. (1983). Tectonique et pétrographie du district à pyrrhotine de Kettara. Univ. Strasbourg.
- Bordonaro, M., Gaillet, J., & Michard, A. (1979). Le géosynclinal carbonifère sud-mésétien dans les Jebilet (Maroc); une corrélation avec la province pyrénéenne du Sud de l'Espagne. *Comptes Rendus de l'Académie des Sciences Paris*, 233, 707–710.
- Bouabdelli, M. (1994). Tectonique de l'Est du Massif hercynien central (zone d'Azrou-Khénifra). *Bulletin Institute Des Sciences, Rabat*, 18, 145–168.
- Bouabdelli, M., & Piqué, A. (1996). Du bassin sur décrochement au bassin d'avant-pays: dynamique du Bassin d'Azrou-Khénifra (Maroc hercynien central). *Journal of African Earth Sciences*, 23(2), 213–224. [https://doi.org/10.1016/S0899-5362\(96\)00063-2](https://doi.org/10.1016/S0899-5362(96)00063-2)
- Bouloton, J. (1992). Mise en évidence de cordiérite héritée des terrains traversés dans le pluton granitique des Ouled Ouaslam (Jebilet, Maroc). *Canadian Journal of Earth Sciences*, 29(4), 658–668. <https://doi.org/10.1139/e92-057>
- Bouloton, J., & Gasquet, D. (1995). Melting and undercooled crystallisation of felsic xenoliths from minor intrusions (Jebilet massif, Morocco). *Lithos*, 35(3–4), 201–219. [https://doi.org/10.1016/0024-4937\(94\)00051-3](https://doi.org/10.1016/0024-4937(94)00051-3)
- Bouloton, J., & Le Corre, C. (1985). Le problème de la tectonique tangentielle dans les Jebilet (Maroc hercynien): données et hypothèses. *Hercynica*, 1, 121–129.
- Boummane, M. H., & Olivier, P. (2007). The Ouled Ouaslam Variscan granitic pluton (Jebilet Massif, Southwestern Moroccan Meseta): A forcibly emplaced laccolithic intrusion characterized by its magnetic and magmatic fabrics. *Journal of African Earth Sciences*, 47(1), 49–61. <https://doi.org/10.1016/j.jafrearsci.2006.10.004>
- Chopin, F., Corsini, M., Schulmann, K., El Houicha, M., Ghienne, J. F., & Edel, J. B. (2014). Tectonic evolution of the Rehamna metamorphic dome (Morocco) in the context of the Alleghanian-Variscan orogeny. *Tectonics*, 33, 1154–1177. <https://doi.org/10.1002/2014TC003539>
- Compston, W., Williams, I. S., Kirschvink, J. L., Zichao, Z., & Guogan, M. A. (1992). Zircon U-Pb ages for the Early Cambrian time-scale. *Journal of the Geological Society*, 149(2), 171–184. <https://doi.org/10.1144/gsjgs.149.2.0171>
- Corsini, M., Cornée, J. J., Muller, J., & Vauchez, A. (1988). Cisaillement ductile synmétamorphe et déplacement tangentiel vers le SW dans les Rehamna (Maroc hercynien). *Comptes Rendus de l'Académie Des Sciences. Série 2, Mécanique, Physique, Chimie, Sciences de l'univers, Sciences de la Terre*, 306(19), 1389–1394.
- Delchini, S., Lahfid, A., Plunder, A., & Michard, A. (2016). Applicability of the RSCM geothermometry approach in a complex tectono-metamorphic context: The Jebilet massif case study (Variscan Belt, Morocco). *Lithos*, 256, 1–12.
- Dostal, J., Keppie, J. D., Hamilton, M. A., Aarab, E. M., Lefort, J. P., & Murphy, J. B. (2005). Crustal xenoliths in Triassic lamprophyre dykes in western Morocco: Tectonic implications for the Rheic Ocean suture. *Geological Magazine*, 142(2), 159–172. <https://doi.org/10.1017/S0016756805000440>
- Edel, J. B., Schulmann, K., Lexa, O., & Lardeaux, J. M. (2018). Late Palaeozoic palaeomagnetic and tectonic constraints for amalgamation of Pangea supercontinent in the European Variscan belt. *Earth-Science Reviews*, 177, 589–612. <https://doi.org/10.1016/j.earscirev.2017.12.007>
- El Hassani, A. (1980). Etude lithostratigraphique, tectonique et pétrographique de la région de Sidi Bou-Othmane (Maroc). Contribution à la connaissance de l'évolution du segment hercynien des Jebilet centrales. Univ. Aix-Marseille.
- Essaifi, A., Capdevila, R., & Lagarde, J. L. (1995). Transformation de leucogabbros en chloritoschistes sous l'effet de l'altération hydrothermale. *Comptes Rendus de l'Académie Des Sciences: Earth & Planetary Sciences. Sciences de La Terre et Des Planètes. Série II*, 320, 189.
- Essaifi, A., Capdevila, R., & Lagarde, J. L. (2004). Metasomatic trondhjemites and tonalites: Examples in Central Jebilet (Hercynian, Morocco). *Journal of African Earth Sciences*, 39(3–5), 369–374. <https://doi.org/10.1016/j.jafrearsci.2004.07.031>
- Essaifi, A., Lagarde, J. L., & Capdevila, R. (2001). Deformation and displacement from shear zone patterns in the Variscan upper crust, Jebilet, Morocco. *Journal of African Earth Sciences*, 32(3), 335–350. [https://doi.org/10.1016/S0899-5362\(01\)90101-0](https://doi.org/10.1016/S0899-5362(01)90101-0)
- Essaifi, A., Potrel, A., Capdevila, R., & Lagarde, J. L. (2003). Datation U-Pb: âge de mise en place du magmatisme bimodal des Jebilet centrales (chaîne Varisque, Maroc). Implications géodynamiques. *Comptes Rendus Geosciences*, 335(2), 193–203. [https://doi.org/10.1016/S1631-0713\(03\)00030-0](https://doi.org/10.1016/S1631-0713(03)00030-0)
- Essaifi, A., Samson, S., & Goodenough, K. (2013). Geochemical and Sr-Nd isotopic constraints on the petrogenesis and geodynamic significance of the Jebilet magmatism (Variscan Belt, Morocco). *Geological Magazine*, 151(4), 666–691. <https://doi.org/10.1017/S0016756813000654>
- Festa, A., Dilek, Y., Pini, G. A., Codegone, G., & Ogata, K. (2012). Mechanisms and processes of stratal disruption and mixing in the development of mélanges and broken formations: Redefining and classifying mélanges. *Tectonophysics*, 568–569, 7–24. <https://doi.org/10.1016/j.tecto.2012.05.021>
- Festa, A., Ogata, K., Pini, G. A., Dilek, Y., & Alonso, J. L. (2016). Origin and significance of olistostromes in the evolution of orogenic belts: A global synthesis. *Gondwana Research*, 39, 180–203. <https://doi.org/10.1016/j.gr.2016.08.002>
- Festa, A., Pini, G. A., Dilek, Y., & Codegone, G. (2010). Mélanges and mélange-forming processes: A historical overview and new concepts. *International Geology Review*, 52(10–12), 1040–1105. <https://doi.org/10.1080/00206810903557704>

- Franke, W. (2014). Topography of the Variscan orogen in Europe: Failed–not collapsed. *International Journal of Earth Sciences*, 103(5), 1471–1499. <https://doi.org/10.1007/s00531-014-1014-9>
- Franke, W., Cocks, L. R. M., & Torsvik, T. H. (2017). The Palaeozoic Variscan oceans revisited. *Gondwana Research*, 48, 257–284. <https://doi.org/10.1016/j.gr.2017.03.005>
- Frizon de Lamotte, D., Tavakoli-Shirazi, S., Leturmy, P., Averbuch, O., Mouchot, N., Raulin, C., et al. (2013). Evidence for Late Devonian vertical movements and extensional deformation in northern Africa and Arabia: Integration in the geodynamics of the Devonian world. *Tectonics*, 32, 107–122. <https://doi.org/10.1002/tect.20007>
- Gaillet, J. (1980). Données sur la lithologie et la tectonique des formations dinantiennes du domaine Sud Mésétien (Jebilet-Haouz et Haut Atlas de Marrakech). *Mines, Géologie et Energie*, 48, 63–67.
- Gaillet, J., & Bordonaro, M. (1981). La tectogenèse hercynienne dans le massif Dinantien des Jebilet centrales (Maroc). *Sciences Géologiques. Bulletin*, 34, 117–122.
- Gaillet, J. L. (1979). Sur les relations entre les Schistes du Sarhlef et le Flysch de Kharrouba dans le massif hercynien des Jebilet (Maroc). *Comptes rendus de l'Académie des Sciences Paris Séries D*, 288, 791–794.
- Ghorbal, B., Bertotti, G., Foeken, J., & Andriessen, P. (2008). Unexpected Jurassic to Neogene vertical movements in stable parts of NW Africa revealed by low temperature geochronology. *Terra Nova*, 20(5), 355–363. <https://doi.org/10.1111/j.1365-3121.2008.00828.x>
- Graham, J. R. (1982a). Transition from basin–plain to shelf deposits in the Carboniferous flysch of Southern Morocco. *Sedimentary Geology*, 33(3), 173–193. [https://doi.org/10.1016/0037-0738\(82\)90054-9](https://doi.org/10.1016/0037-0738(82)90054-9)
- Graham, J. R. (1982b). Wave-dominated shallow-marine sediments in the Lower Carboniferous of Morocco. *Journal of Sedimentary Research*, 52(4), 1271–1276.
- Hafid, M. (2006). Styles structuraux du Haut Atlas de Cap Tafelney et de la partie septentrionale du Haut Atlas occidental: tectonique salifère et relation entre l'Atlas et l'Atlantique. *Notes et Mémoire Du Service Géologique Du Maroc*, 465, 172.
- Hafid, M., Tari, G., Bouhadioui, B., El Moussaid, I., Echcharfaoui, H., Ait Salem, A., et al. (2008). Atlantic Basins. In *Continental evolution: The geology of Morocco* (pp. 301–329). Berlin: Springer.
- Hatcher, R. D. (2002). Alleghanian (Appalachian) orogeny, a product of zipper tectonics: Rotational transpressive continent–continent collision and closing of ancient oceans along irregular margins. *Special Paper-Geological Society of America*, 364, 199–208.
- Hatcher, R. D. (2010). The Appalachian orogen: A brief summary. *Geological Society of America Memoirs*, 206, 1–19. [https://doi.org/10.1130/2010.1206\(01\)](https://doi.org/10.1130/2010.1206(01))
- Hoepffner, C., Houari, M. R., & Bouabdelli, M. (2006). Tectonics of the North African Variscides (Morocco, western Algeria): An outline. *Comptes Rendus Geoscience*, 338(1–2), 25–40. <https://doi.org/10.1016/j.crte.2005.11.003>
- Hoepffner, C., Soulaïmani, A., & Piqué, A. (2005). The Moroccan Hercynides. *Journal of African Earth Sciences*, 43(1–3), 144–165. <https://doi.org/10.1016/j.jafrearsci.2005.09.002>
- Hollard, H., Huvelin, P., & Mamet, B. (1977). Stratigraphie du Viséen supérieur des Jebilet et âge de la mien place de la Nappe des Jebilet orientales (Maroc). *Notes Service Géologique Maroc*, 37(267), 7–22.
- Huvelin, P. (1977). Etude géologique et géologique du Massif hercynien des Jebilet (Maroc occidental). *Notes Mém Serv Géol Maroc* (Vol. 232 bis).
- Izart, A., Beauchamp, J., Vachard, D., Tourani, A. I., & Essamani, M. (1997). Stratigraphie séquentielle du Carbonifère inférieur du haut Atlas central et des Jebilet (Maroc): un exemple de bassins à turbidites contrôlées par la tectonique. *Journal of African Earth Sciences*, 24(4), 445–454. [https://doi.org/10.1016/S0899-5362\(97\)00074-2](https://doi.org/10.1016/S0899-5362(97)00074-2)
- Jadid, M. (1989). Etude des processus de différenciation des roches magmatiques pré-organiques des Jbilet centrales sur l'exemple du massif stratiforme de Koudiat Kettara (Maroc Hercynien). Marrakech: Univ. Cadi Ayyad, Faculté des Sciences–Semlalia.
- Kroner, U., Roscher, M., & Romer, R. L. (2016). Ancient plate kinematics derived from the deformation pattern of continental crust: Paleo- and Neo-Tethys opening coeval with prolonged Gondwana–Laurussia convergence. *Tectonophysics*, 681, 220–233. <https://doi.org/10.1016/j.tecto.2016.03.034>
- Lagarde, J. L. (1985). Cisaillements ductiles et plutons granitiques contemporains de la déformation hercynienne post-viséenne de la Meseta marocaine. *Hercynica*, 1(1), 29–37.
- Lagarde, J. L., Ait Ayad, N., Ait Omar, S., Chemsseddoha, A., & Saquaque, A. (1989). Les plutons granitiques tardi carbonifères marqueurs de la déformation crustale. L'exemple des granitoïdes de la méséta marocaine. *Comptes Rendus de l'Académie Des Sciences*, 309(3), 291–296.
- Lagarde, J. L., & Choukroune, P. (1982). Cisaillement ductile et granitoïdes syntectoniques l'exemple du massif hercynien des Jebilet. *Bulletin de la Société Géologique de France*, 24(2), 299–307.
- Le Corre, C., & Bouloton, J. (1987). Un modèle de "structure en fleur" associant décrochement et convergence: les Jebilet centro-occidentales (Maroc hercynien). *Comptes rendus de l'Académie des Sciences Paris*, 304(13), 751–754.
- Le Corre, C., & Saquaque, A. (1987). Comportement d'un système pluton–encaissant dans un champ de déformation regional; le granite du Bramram (Jebilet, Maroc hercynien). *Bulletin de la Société Géologique de France*, 3(4), 665–673.
- Ludwig, K. R. (2003). User's manual for Isoplot 3.00: a geochronological toolkit for Microsoft Excel. Kenneth R. Ludwig.
- Marcoux, E., Belkabar, A., Gibson, H. L., Lentz, D., & Ruffet, G. (2008). Draa Sfar, Morocco: A Visean (331 Ma) pyrrhotite-rich, polymetallic volcanic massive sulphide deposit in a Hercynian sediment-dominant terrane. *Ore Geology Reviews*, 33(3–4), 307–328. <https://doi.org/10.1016/j.oregeorev.2007.03.004>
- Mayol, S. (1987). Géologie de la partie occidentale de la boutonnière paléozoïque des Jebilet, Maroc: un exemple d'évolution structurale hercynienne de bassins intercontinentaux cambrien et carbonifère. Faculté des sciences Saint-Jérôme, Laboratoire de géologie dynamique.
- Michard, A., Hoepffner, C., Soulaïmani, A., & Baïdder, L. (2008). The Variscan Belt. In *Continental evolution: The geology of Morocco* (pp. 65–132). Berlin: Springer.
- Michard, A., Soulaïmani, A., Hoepffner, C., Ouanaïmi, H., Baïdder, L., Rjmati, E. C., & Sadiqi, O. (2010). The South-Western Branch of the Variscan Belt: Evidence from Morocco. *Tectonophysics*, 492(1–4), 1–4. <https://doi.org/10.1016/J.TECTO.2010.05.021>
- Moreno, C., Sáez, R., González, F., Almodóvar, G., Toscano, M., Playford, G., et al. (2008). Age and depositional environment of the Draa Sfar massive sulfide deposit, Morocco. *Mineralium Deposita*, 43(8), 891–911. <https://doi.org/10.1007/s00126-008-0199-x>
- Mrini, Z., Rafi, A., Duthou, J. L., & Vidal, P. (1992). Chronologie Rb–Sr des granitoïdes hercyniens du Maroc: conséquences. *Bulletin de la Société Géologique de France*, 163(3), 281–291.
- Nance, R. D., Gutiérrez-Alonso, G., Keppie, J. D., Linnemann, U., Murphy, J. B., Quesada, C., et al. (2010). Evolution of the Rheic ocean. *Gondwana Research*, 17(2–3), 194–222. <https://doi.org/10.1016/j.gr.2009.08.001>

- Nance, R. D., Gutiérrez-Alonso, G., Keppie, J. D., Linnemann, U., Murphy, J. B., Quesada, C., et al. (2012). A brief history of the Rheic Ocean. *Geoscience Frontiers*, 3(2), 125–135. <https://doi.org/10.1016/j.gsf.2011.11.008>
- Piqué, A. (1979). Evolution structurale d'un segment de la chaîne hercynienne: la Meseta marocaine nord occidentale. Univ. Strasbourg.
- Piqué, A., Jeannette, D., & Michard, A. (1980). The Western Meseta Shear Zone, a major and permanent feature of the Hercynian belt in Morocco. *Journal of Structural Geology*, 2(1–2), 55–61. [https://doi.org/10.1016/0191-8141\(80\)90034-6](https://doi.org/10.1016/0191-8141(80)90034-6)
- Piqué, A., & Michard, A. (1989). Moroccan Hercynides: A synopsis: The Paleozoic sedimentary and tectonic evolution at the northern margin of West Africa. *American Journal of Science*, 289(3), 286–330. <https://doi.org/10.2475/ajs.289.3.286>
- Playford, G., González, F., Moreno, C., & Alansari, A. (2008). Palynostratigraphy of the Sarhlef Series (Mississippian), Jebilet Massif, Morocco. *Micropaleontology*, 54(2), 89–124.
- Ramsay, J. G. (1967). *Folding and fracturing of rocks* (p. 568). New York: Mc Graw Hill Book Company.
- Roddaz, M., Brusset, S., Soula, J. C., Béziat, D., Ben Abbou, M., Debat, P., et al. (2002). Foreland basin magmatism in the Western Moroccan Meseta and geodynamic inferences. *Tectonics*, 21(5), 1043. <https://doi.org/10.1029/2001TC901029>
- Rosé, F. (1987). Les types granitiques du Maroc hercynien. Univ. Paris VI.
- Saddiqi, O., el Haimer, F. Z., Michard, A., Barbarand, J., Ruiz, G. M. H., Mansour, E. M., et al. (2009). Apatite fission-track analyses on basement granites from south-western Meseta, Morocco: Paleogeographic implications and interpretation of AFT age discrepancies. *Tectonophysics*, 475(1), 29–37. <https://doi.org/10.1016/j.tecto.2009.01.007>
- Schulmann, K., Schaltegger, U., Jezek, J., Thompson, A. B., & Edel, J.-B. (2002). Rapid burial and exhumation during orogeny: Thickening and synconvergent exhumation of thermally weakened and thinned crust (Variscan orogen in Western Europe). *American Journal of Science*, 302(10), 856–879. <https://doi.org/10.2475/ajs.302.10.856>
- Simancas, J. F., Azor, A., Martínez-Poyatos, D., Tahiri, A., el Hadi, H., González-Lodeiro, F., et al. (2009). Tectonic relationships of Southwest Iberia with the allochthons of Northwest Iberia and the Moroccan Variscides. *Comptes Rendus Geoscience*, 341(2–3), 103–113. <https://doi.org/10.1016/j.crte.2008.11.003>
- Sláma, J., Košler, J., Condon, D. J., Crowley, J. L., Gerdes, A., Hanchar, J. M., et al. (2008). Plešovice zircon—A new natural reference material for U–Pb and Hf isotopic microanalysis. *Chemical Geology*, 249(1), 1–35.
- Sougy, J. (1976). Existence d'une importante tectonique tangentielle avec nappes repliées, dans les Jebilet occidentales et centrales, Méséta marocaine hercynienne: rapport de tournée, mars 1976. Laboratoire de géologie dynamique.
- Tahiri, A. (1982). Lithostratigraphie, structure et métamorphisme de la partie sud des Jebilet occidentales autochtones et allochtones. Univ. Aix-Marseille.
- Tera, F., & Wasserburg, G. J. (1972). U–Th–Pb systematics in three Apollo 14 basalts and the problem of initial Pb in lunar rocks. *Earth and Planetary Science Letters*, 14(3), 281–304. [https://doi.org/10.1016/0012-821X\(72\)90128-8](https://doi.org/10.1016/0012-821X(72)90128-8)
- Thompson, A. B., Schulmann, K., Jezek, J., & Tolar, V. (2001). Thermally softened continental extensional zones (arcs and rifts) as precursors to thickened orogenic belts. *Tectonophysics*, 332(1–2), 115–141. [https://doi.org/10.1016/S0040-1951\(00\)00252-3](https://doi.org/10.1016/S0040-1951(00)00252-3)
- Tisserant, D. (1977). Les isotopes du strontium et l'histoire hercynienne du Maroc. Etude de quelques massifs atlasiques et mésétiens. Univ. Strasbourg.
- Wernert, P., Schulmann, K., Chopin, F., Štípská, P., Bosch, D., & El Houicha, M. (2016). Tectonometamorphic evolution of an intracontinental orogeny inferred from P–T–t–d paths of the metapelites from the Rehamna massif (Morocco). *Journal of Metamorphic Geology*, 34(9), 917–940. <https://doi.org/10.1111/jmg.12214>
- Wiedenbeck, M., Alle, P., Corfu, F., Griffin, W. L., Meier, M., Oberli, F. V., et al. (1995). Three natural zircon standards for U–Th–Pb, Lu–Hf, trace element and REE analyses. *Geostandards and Geoanalytical Research*, 19(1), 1–23. <https://doi.org/10.1111/j.1751-908X.1995.tb00147.x>
- Youbi, N., Bellon, H., Marzin, A., Piqué, A., Cotten, J., & Cabanis, B. (2001). Du cycle orogénique hercynien au pré-rifting de l'Atlantique central au Maroc occidental: les microdiorites des Jbilet sont-elles des marqueurs magmatiques de ce passage? *Comptes Rendus de l'Académie des Sciences - Series IIA - Earth and Planetary Science*, 333(5), 295–302. [https://doi.org/10.1016/S1251-8050\(01\)01643-3](https://doi.org/10.1016/S1251-8050(01)01643-3)
- Zahraoui, M. (1981). Etude lithostratigraphique et structurale des nappes de la région du Jbel Tekzim (Jebilet centrales, Maroc): contribution à la connaissance de l'évolution de la chaîne hercynienne de la Meseta marocaine, (Thèse de 3ème Cycle). Univ. Aix-Marseille.